

THE ROLE OF SLOW-TWITCH SKELETAL MUSCLE IN
THE MUSCULOSKELETAL ENDOCRINE AXIS

A THESIS IN
Cellular and Molecular Biology

Presented to the Faculty of the University
of Missouri-Kansas City in partial fulfillment of
the requirements for the degree

MASTER OF SCIENCE

by
JULIAN A. VALLEJO

B.S., University of Missouri-Kansas City, 2011

Kansas City, Missouri
2016

THE ROLE OF SLOW-TWITCH SKELETAL MUSCLE IN THE MUSCULOSKELETAL ENDOCRINE
AXIS

Julian A. Vallejo, Candidate for the Master of Science Degree in Cellular and Molecular
Biology

University of Missouri-Kansas City, 2016

ABSTRACT

In addition to coupling mechanically to produce movement, the musculoskeletal unit has an endocrine function, capable of signaling to distant tissues as well as locally through the release of hormone-like molecules. Musculoskeletal disuse triggers loss of bone and skeletal muscle function while exercise improves musculoskeletal health and protects against chronic disease. We investigated potential crosstalk pathways within the musculoskeletal unit involving, (1) muscle derived BAIBA in muscle-to-bone crosstalk and (2) bone MBTPS1 in bone-to-muscle crosstalk. To assess the impact of BAIBA on muscle and bone properties, mice were immobilized for two weeks via hind limb suspension while receiving L-BAIBA. Fast twitch extensor digitorum longus (EDL) muscles and slow twitch soleus muscles were then isolated for *ex vivo* contractility testing and tibia was obtained for analysis of trabecular bone content. In muscle, L-BAIBA supplementation showed no effect on muscle mass or EDL contractile function but increased slow-twitch soleus

contractile force by 15% over non-supplemented mice. In addition, the rate of soleus muscle contractile force development was greater in the supplemented group compared to control. In bone, L-BAIBA receiving mice had higher tibia BV/TV compared to control. Next, we investigated the role of *Mbtps1* in bone-to-muscle crosstalk using osteocyte-specific *Mbtps1* conditional knock-out mouse (cKO) using *Dmp1*-driven Cre. MBTPS1 is a widely expressed proprotein convertase involved in proprotein processing within the secretory pathway. In bone, MBTPS1 is required for normal skeletal development and mineralization. *Ex vivo* contractility of cKO EDL and soleus muscles revealed an age-related enhancement of slow-twitch soleus muscle contractile force, muscle size and regeneration of slow type-1 muscle fibers compared to control littermates while EDL muscle properties remained largely unaffected. Subsequent gene array analysis uncovered upregulation of genes related to muscle contraction, oxidative metabolism and muscle regeneration in the cKO soleus. These findings reveal possible targeted impacts of musculoskeletal auto-, para-, and endocrine signaling among slow twitch skeletal muscle and support the novel paradigm of relevant musculoskeletal crosstalk axes in the maintenance of muscle and bone health.

APPROVAL PAGE

The faculty listed below, appointed by the Dean of the School Biological Sciences have examined a thesis titled "The Role of Slow-Twitch Skeletal Muscle in the Musculoskeletal Endocrine Axis," presented by Julian A. Vallejo, candidate for the Master of Science in Cellular and Molecular Biology degree, and certify that in their opinion it is worthy of acceptance.

Supervisory Committee

Lynda F. Bonewald, Ph.D., Committee Chair
Department of Oral and Craniofacial Sciences, School of Dentistry

Michael J. Wacker, Ph.D.
Department of Basic Medical Science, School of Medicine

Anthony Persechini, Ph.D.
Department of Molecular Biology and Biochemistry, School of Biological Sciences

Saul M. Honigberg, Ph.D.
Department of Cell Biology and Biophysics, School of Biological Sciences

CONTENTS

ABSTRACT	iii
LIST OF ILLUSTRATIONS	ix
LIST OF TABLES.....	x
Chapter	
1. INTRODUCTION	1
Skeletal Muscle Heterogeneity.....	1
Muscle-Bone Interaction	2
Mechanosensation and Transduction	2
Musculoskeletal Unloading/Disuse	3
Skeletal Muscle as a Secretory Organ	4
β -aminoisobutyric Acid (BAIBA): A Metabolite Exercise Factor	6
Bone as a Secretory Organ	7
The Proprotein Convertase MBTPS1	9
2. METHODOLOGY	11
BAIBA Study	11
Muscle Conditioned Media (MCM)	11
Quantitation of BAIBA Isomers in MCM	11
Hind limb Unloading	13
<i>Ex Vivo</i> Muscle Contractility at Physiological Temperature	13

<i>Ex Vivo</i> Microcomputed Tomography (μ CT).....	15
MBTPS1 Study	15
<i>Dmp1-cre Mbtps1 cKO Mice</i>	15
<i>Ex Vivo</i> Muscle Contractility at Room Temperature	16
Immunohistochemistry of Muscle Cryosections	18
Muscle RNA Isolation and Processing for Whole Genome Array.....	19
Statistics	20
3. RESULTS.....	21
BAIBA Study	21
L-BAIBA but Not D-BAIBA is Released from Isolated Contracting Skeletal Muscles	21
L-BAIBA Supplementation Maintains Contractile Force in Soleus Muscles During Unloading	23
L-BAIBA Does Not Affect Muscle Dependence on Extracellular Ca ²⁺ or Fatigue/Recovery from Fatigue	27
Preserved Tibial Trabecular Bone Volume in Mice Supplemented With L-BAIBA	29
MBTPS1 Study	30
Soleus Muscles but Not EDL Muscles from Adult <i>Mbtps1</i> cKO Mice Are Larger and Produce More Contractile Force	30
Soleus Muscles from Adult <i>Mbtps1</i> cKO Mice Display Rightward Shift of the Force-Frequency Relationship	32
Type 1 Myosin Heavy Chain-Expressing cKO Soleus Muscle Myofibers Exhibit Centralized Nuclei	34

Contractile Properties of Soleus and EDL Muscles from 3-Month Old <i>Mbtps1</i> cKO Mice	35
Whole Genome Array of cKO Soleus Muscles Provides Clues for Increased Performance	37
4. DISCUSSION	39
REFERENCES CITED	48
VITA.....	56

ILLUSTRATIONS

Illustration	Page
1. <i>Ex Vivo</i> Contractility Methodology	22
2. LC/MS Quantification of L-BAIBA in MCM	22
3. <i>Ex Vivo</i> Contractility of Hind Limb Suspended Soleus Muscle.....	25
4. <i>Ex Vivo</i> Contractility of Hind Limb Suspended EDL Muscle	26
5. Soleus Muscle Dependence on External Ca ²⁺ and Fatigue/Recovery Properties	28
6. Bone Content of Hind Limb Suspended Mice.....	29
7. Muscle Size and Contractile Force of 10 Month-Old <i>Mbtphs1</i> cKO Mice.	31
8. Contractile Properties of 10 Month-Old <i>Mbtphs1</i> cKO Mice	33
9. Immunostaining of Soleus Cryosections.....	35
10. Contractile Properties of 3 Month-Old <i>Mbtphs1</i> cKO Mice	36

TABLES

Table	Page
1. Whole Genome Array	38

CHAPTER 1

INTRODUCTION

Skeletal Muscle Heterogeneity

The musculoskeletal unit plays dual roles in providing the mechanical components for physical activity as well as functioning as an endocrine organ regulating distant and local tissue physiology. Skeletal muscles comprise the largest organ system in the body with each muscle constituting a mosaic of different myofiber types with distinct mechanical and metabolic properties, the relative proportions of which equate to a specific whole muscle functional output. The relationship of muscle fiber type and contractile function was initially described in frog (*Rana pipiens* & *R. catesbeiana*) in the 1950's where it was observed that certain fiber populations displayed "tonic" or rapid contractile responses while other fibers showed a "phasic" or prolonged contractile response to nerve stimulation (1). Subsequent studies provided the physiological evidence to suggest that sarcomeric myosin, the molecular motor underlying contraction, existed as several isoforms confined to specific fiber types within muscle (2, 3) and that contractile force and shortening velocity directly correlated with the distinct myosin heavy chain (MHC) isoform expression profiles (4). Among these, MHC type 1 (MHC1) expressing fibers or "slow twitch" fibers display reduced contractile force and slower shortening velocity relative to MHC type 2 (MHC2) enriched or "fast twitch" fibers. The contribution of the MHC isoforms to muscle contraction velocity is attributed to rate of ADP release from the MHC-ATPase catalytic domain during the power stroke step of the cross bridge cycle. MHC1 exhibits the

lowest rate of ADP dissociation relative to MHC2 isoforms which increase in release rate in order from MHC2a \rightarrow 2x \rightarrow 2b (5). Additional fiber-type specific myofibrillar and calcium handling protein isoforms that contribute to a fast or slow myofiber phenotype include fast/slow myosin light chain isoforms and phosphorylation state (6), troponin, tropomyosin and sarcoplasmic/endoplasmic reticulum Ca^{2+} ATPase (SERCA) (7).

Muscle fiber types may be further subcategorized with respect to metabolic character. These subcategories include slow twitch oxidative (e.g. Soleus muscle), fast twitch oxidative (e.g. Semitendinosus muscle) or fast twitch glycolytic muscles (e.g. Extensor digitorum longus muscle). Oxidative muscles harbor abundant mitochondria, increased vascularization and a higher content of the O_2 binding protein myoglobin, conferring the advantage of increased resistance to muscle fatigue during endurance activity (8). In addition to generating mobility, muscle contraction also plays an important role in the regulation of bone physiology.

Muscle-Bone Interaction

Mechanosensation and Transduction

The intimate and co-regulatory relationship of skeletal muscle and bone beyond the manifestation of physical movement has been known for quite some time wherein physical load placed on bone related to muscle contractile forces, serves as a signal to which the main resident cells of mineralized bone, the osteocytes, are able to sense and respond by modulation of bone architecture and mass (9). Osteocytes reside within cavities embedded in the mineralized bone matrix, termed lacunae, which provide the osteocyte with oxygen and nutrients via a network of small canals linked to the vasculature and other

osteocyte lacunae called the lacunar-canalicular system (10). There is evidence to suggest that osteocytes sense mechanical loading through the shear stress produced by movement of the surrounding canalicular fluid triggering an anabolic paracrine response within bone. This response is characterized by initial release of bone anabolic mediator molecules from osteocytes including ATP, nitric oxide (NO) and prostaglandin E2 (PGE2) which may also travel to neighboring osteocytes through gap junctions or be secreted into the bone fluid (11, 12).

Musculoskeletal Unloading/Disuse

Lack of applied load on bone such as with prolonged inactivity of muscle during bed rest or in a microgravity environment such as space flight, results in dramatic alterations in the structure and function of the musculoskeletal unit. The response to reduced loading in bone leads to a compromised ability to form new bone and increases bone resorption activity of osteoclasts, equating to a total net loss of cortical and trabecular bone content and diminished bone strength (13, 14). In the case of muscle, disuse triggers significant muscle atrophy, reduced muscle fiber cross sectional area (CSA), and lowered muscle contractile force and fatigue resistance. The adaptive response to unloading manifests chiefly and initially and in the slow twitch muscles like the soleus (14-16), while predominately fast twitch muscles such as the extensor digitorum longus (EDL) muscle tend to resist this transformation (15). The adaptation of slow twitch muscles to disuse is underscored by the modification of muscle fiber type and metabolic homeostasis including a shift in MHC composition from the slower type 1 to faster type 2 MHC isoforms (17) concomitant with the degradation of oxidative metabolic capacity. Mitochondrial

dynamics and function show a compromised fate following muscle disuse highlighted by a reduction in mitochondrial biogenesis (18, 19), altered mitochondrial morphology (20), and lowered respiratory potential (21, 22). The physiological response of the musculoskeletal unit to extended physical inactivity not only impacts the quality of muscle and bone but is also associated with an increased risk for the development of chronic diseases such as obesity, type II diabetes mellitus, cardiovascular disease and cancer (23, 24). It is becoming more apparent that the influence of muscle activity and exercise on long term systemic health outcomes may therefore rely on alternate avenues of communication consisting of biochemical and hormonal interaction among muscle and distant organs.

Skeletal Muscle as a Secretory Organ

The discovery that skeletal muscles function as a secretory organ by releasing signaling molecules (termed “myokines” by the Pederson laboratory) in response to exercise (25) and that these factors may confer health benefits has sparked great interest from a therapeutic perspective (26). Myokines may exert their effects in an auto-, para- or endocrine manner within the body. The foremost identified and utmost studied myokine is Interluekin-6 (IL-6). Originally observed to increase 100-fold in plasma following muscular exercise (27), IL-6 release and signaling is independent of contraction-induced muscle damage (28, 29) and has been shown to offer protection against obesity and type 2 diabetes by enhancing fatty acid oxidation and glucose uptake in local muscle beds (30) and distant organs such as adipose tissue (27) and liver (31) via an AMP-activated protein kinase (AMPK) mediated pathway. In contrast to the pro-inflammatory response associated with IL-6 release from circulating immune cells like monocytes, IL-6 derived from muscle activity

actually leads to increased content of circulating anti-inflammatory interleukin1 receptor antagonist (IL-1ra) and IL-10 which ease whole-body inflammation after a single bout of exercise (32, 33). Additional interleukin-type myokines discovered to date include IL-7, 8, and 15 which are involved in diverse adaptive processes such as angiogenesis (34, 35) myogenic differentiation (36) and muscle hypertrophy (37). Interestingly, overproduction of muscle IL-15 in transgenic mice led to augmented bone mineral density (38). Further evidence suggests the existence of additional and important endocrine communication axes between skeletal muscle and bone.

Additional myokines so far identified and associated with effects in bone include myostatin and irisin. Myostatin, a member of the TGF- β superfamily is synthesized and released into the circulation by muscle where it primarily acts locally as a negative regulator of muscle mass. Circulating myostatin levels have been observed to be inversely associated with bone mineral density and bone content in rodents and humans (39). Next, the exercise-induced peptide myokine irisin, is currently the focus of considerable research for its potential in treatment/prevention of metabolic diseases. Irisin is the cleavage product of the myo-membrane protein fibronectin type III domain containing peptide 5 (FNDC5) which is secreted into the vasculature in a pattern dependent upon the exercise response master transcriptional regulator, peroxisome proliferator-activated receptor- γ coactivator-1 α (PGC-1 α) (40). Irisin alters metabolic homeostasis through stimulation of fatty acid β -oxidation and induction of a brown fat-like phenotype in white adipose tissue through upregulation of genes involved in thermogenesis like uncoupling protein 1 (*Ucp1*) (41). In bone, irisin has been demonstrated to produce anabolic effects on cortical bone formation by driving

expression of key osteogenic genes such as *Runx2*, *Osx*, and β -catenin while downregulating the osteogenic inhibitor, *Sost* (42, 43). Secreted metabolic regulatory factors such as irisin may form a crucial endocrine crosstalk pathway linking muscle and bone health. The newly identified small molecule exercise factor, β -aminoisobutyric acid (BAIBA) has been found to modulate systemic energy homeostasis in response to exercise and may also mediate the positive effects of exercise on the musculoskeletal unit.

β -aminoisobutyric Acid (BAIBA): A Metabolite Exercise Factor

BAIBA is a non-proteinogenic β -amino acid produced during catabolism of thymine and valine. BAIBA was initially observed to exert reducing effects on body adiposity which stemmed from the observation that certain thymine analogue antiretroviral reverse transcriptase inhibitors (stavudine, zidovudine) induced significant fat wasting in mice leading to a significant reduction in fat mass while lean mass remained unaltered (44). Upon evaluation of the catabolites of these drugs, BAIBA was found to recapitulate the fat wasting effects by reducing body adiposity through enhancing hepatic mitochondrial fatty acid oxidation and downregulating *de novo* lipidogenesis in normal and obese mice (44, 45) suggesting an exciting new potential as an anti-obesity treatment. A recent study utilizing a metabolic profiling technique to identify novel muscle secreted metabolites participating in exercise-related tissue crosstalk, identified an enrichment of BAIBA in conditioned media from myocytes overexpressing PGC-1 α (46). The authors went on to show that following wheel running exercise in mice, serum levels of BAIBA were increased. Furthermore, application of BAIBA to isolated primary inguinal adipocytes and *in vivo* showed an increase in expression of the brown adipose specific genes, cell death inducing DFA like effector A

(*Cidea*) and *Ucp1*, and also enhanced cellular respiration and glucose uptake (46). BAIBA has also been demonstrated to attenuate insulin resistance, alleviate hepatic steatosis and reduce hepatic endoplasmic reticulum (ER) stress and apoptosis in a mouse model for type II diabetes (47). Moreover, in skeletal muscle BAIBA administration reversed hyperlipidemic-induced insulin intolerance through AMPK-PPAR δ mediated pathway and suppressed inflammation by inhibiting nuclear factor $\kappa\beta$ (NF $\kappa\beta$) translocation and downstream inflammatory cytokines (48). Indeed, BAIBA-mediated crosstalk pathways harbor potential as treatment targets for metabolic disorders, however it is unknown whether BAIBA may offer similar benefits in the treatment of musculoskeletal diseases such as sarcopenia and osteoporosis.

Bone as a Secretory Organ

Having established a role of skeletal muscle in inter-tissue biochemical communication we now turn to skeletal bone, specifically the main resident cells of bone, osteocytes, and their role in endo-, para-, autocrine signaling. Osteocytes have historically been perceived as passive entities buried deep within the mineralized tissue of bone. However, only recently has the dynamic secretory/endocrine nature of these multifunctional cells and their key involvement in local and non-bone tissue regulation been appreciated (49, 50). Osteocytes are indispensable for the coordination of bone remodeling processes in response to mechanical load through the regulation of both osteoclast and osteoblast activity. As aforementioned, mechanical strain placed upon bone induces the rapid synthesis and release of NO and PGE2 from osteocytes. These secreted factors act to support bone formation by promoting osteoblast differentiation and reducing

proliferative activity (51-53). Osteocytes also secrete several direct inhibitors of bone formation, namely SOST (54), DKK1 (55) and SFRP1 (56) which disrupt the Wnt/β-catenin signaling pathway important for bone anabolism. Osteoclasts are the chief resorbing cells within bone and are activated upon stimulation of receptor-activator of nuclear factor κβ (RANK) through RANK ligand (RANKL). Expression of RANKL has been detected in osteocytes (57) as well as the osteoclast-inducing macrophage colony-stimulating factor (M-CSF) (57) and decoy receptor osteoprotegerin, implicating osteocytes as crucial directors on bone resorption. Osteocytes coordinate with distant tissues such as with the renal system to regulate serum phosphate levels through the actions of osteocyte-derived circulating fibroblast growth factor 23 (FGF23) (58). Circulating FGF23 downregulates sodium/phosphate co-transporters in kidney leading to increased serum phosphate. Interestingly, chronically elevated FGF23 may lead to pathology such as chronic kidney disease, hypo-phosphatemic rickets and even cardiovascular dysfunction (59-63).

Osteocyte-derived factors may also have important implications for skeletal muscle health and homeostasis. Osteocyte/osteoblast-specific deletion of connexin43 led to impaired postnatal muscle development and reduced strength in mice possibly involving circulating osteocalcin (64). Mo and colleagues showed that muscle cells co-cultured with conditioned media from osteocytes or with PGE2 developed into larger myotubes and showed upregulation of key genes involved in myogenic differentiation, mitochondrial homeostasis and intracellular calcium handling (65). Clearly, muscle and bone are in conversation.

The Proprotein Convertase MBTPS1

Subtilisin/kexin isozyme-1 (MBTPS1, SKI-1, S1P) is a widely expressed serine protease belonging to the family of proprotein convertases (PC) which function in proprotein processing within the secretory pathway of cells (66). PCs cleave within specific amino acid consensus sequences in diverse substrates molecules such as prohormones, pro-cytokines and pathogens converting them into biologically active/inactive forms (67, 68). MBTPS1 is mainly localized to the cis/medial Golgi compartment and specifically cleaves peptides at non-basic consensus sequences containing serine, threonine or leucine residues (69).

MBTPS1 has been shown to enzymatically regulate membrane cholesterol content through cleavage of sterol regulatory element binding proteins (SREBPs) (70) as well as regulate cAMP response element-binding protein (CREB) (71) activity. In bone, MBTPS1 is required for normal skeletal development and ossification (72) as loss of function of MBTPS1 results in phenotypic abnormalities to sacral/lumbar vertebrae form and quantity resembling caudal regression syndrome (73). Moreover, osteoblast-directed bone mineralization *in vitro* is dependent upon SK1-1 activity through regulation of mineralization and matrix-related genes, *PheX*, *Dmp1*, fibronectin, tenascin, fibrillin, *Col11a1* and *Col1a2* by MBTPS1-activated transcription factors SERBP and CREB/ATF (74, 75). These results firmly establish a fundamental role for MBTPS1 in the proper development of functional bone.

In summary, based on the secretory role for muscle and bone beyond mechanical interaction, we chose to investigate two potential crosstalk pathways between muscles and bone that of the muscle factor BAIBA and the bone protease, MBTPS1. Firstly, the muscle derived exercise factor, BAIBA, displays autocrine/paracrine and endocrine effects in

muscle, adipose and liver tissues with the potential to treat metabolic disease, however the actions of BAIBA on skeletal muscle contractile function and bone architecture remains to be established. Utilizing a mouse hind limb suspension approach as a model of prolonged hind limb unloading/disuse we hypothesized that BAIBA supplementation would serve as an endogenous exercise signal and attenuate disuse-related muscle and bone functional and structural decline through improvement of contractile force and fatigueability of fast and slow twitch skeletal muscle and reduction of trabecular bone volume loss. We show that supplementation of L-BAIBA within this context resulted in improved sub-maximal contractile force in slow twitch soleus muscle and increased trabecular bone volume. Secondly, we investigated the role of the protease, MBTPS1 in bone-muscle crosstalk. Since MBTPS1 is required for proper processing and release of secreted peptides necessary for bone mineralization, we investigated whether the conditional deletion *in vivo* in the late embedding osteocyte through a *Dmp1-cre X Mbtps1^{f/f}* driven system in 3-month and 10-12 month-old mice would impact skeletal muscle functional properties and size involving a similar secretory mechanism. Here we provide compelling evidence that MBTPS1 mediates a bone-to-muscle crosstalk pathway through repression of myogenesis since its conditional deletion in osteocytes resulted in a slow-twitch muscle-specific increase in soleus muscle mass, contractile force and actively regenerating slow-twitch muscle fibers with age (76).

CHAPTER 2

METHODOLOGY

BAIBA Study

Muscle Conditioned Media (MCM)

Intact EDL and soleus muscles were dissected from 5-month old male and female C57BL/6 mice and stimulated to contract *ex vivo* as previously described (77, 78). Briefly, dissected muscles were ligated via the tendons inside glass chambers containing Ringer's solution. To produce static MCM, muscles were maintained in buffer without contraction for 30 minutes after which point the Ringer's solution was collected and replaced with fresh solution. A length-force relationship was then employed to determine optimal length at which maximal force is achieved. Muscles were equilibrated for 30 min to mimic conditions of normal activity. Following equilibration, muscles were stimulated with frequencies ranging from 1–130 Hz to generate the force versus frequency relationship and to determine the frequency producing maximal force. The bathing solution was then removed and muscles were rinsed with fresh solution to eliminate factors released during the mounting and stretching procedure. To create contracted MCM, muscles were stimulated to contract with a 90Hz stimulus repeated every minute (non-fatiguing) for 30 min after which period the bathing solution was collected.

Quantitation of BAIBA Isomers in MCM

1 ml of MCM containing 3 ml of 10mM D-alanine were concentrated by freeze dry and resolved in 50 ml of A buffer (HPLC-grade water/0.1% Formic Acid). Marfey's

derivatization was performed as described previously with slight modifications (79, 80). Briefly, 20 ml of the resolved pellet was derivatized with 20 ml of 40mM Marfey reagent (Sigma-Aldrich) and 5 ml of 1M triethylammonium (TEA, Sigma-Aldrich) by incubation at 37C for 2.5 hrs. 5 ml of 1M HCl and 150 ml of B buffer (HPLC-grade water/25% Acetonitrile/0.2% Formic Acid) were added to quench the reaction and then analyzed by liquid chromatography-mass spectrometry (LC/MS). Chromatographic separations were performed on a Nucleodur 100-3 C8 column 125 x 2 mm (Macherey–Nagel, Bethlehem, PA) at with flow rate of 0.3 mL/min. The mobile phases consisted of A – water/0.1 % formic acid, B – 70/30/0.1 % acetonitrile/water/formic acid, C – acetonitrile/0.1 % formic acid. Two gradients were used in this study. The long gradient consists of 25 % B for 5 min, 25-42.5 % B over 35 min, 42.5- 25 %B over 1 min, and a post run equilibration time for 4 min. For short method, isocratic 42.5 %B is ran for 15min with a quick wash with 100 %B for 1 min followed by post –equilibrium to 42.5 % B. The long method is to ensure all the BAIBA isomers are separated and short method is to perform quick analysis of muscle CM. Mass spectrometry quantitation was performed using selection reaction monitoring (SRM) detection in positive mode for Marfey's derivatized BAIBA isomers. The Q1 (parent mass) is 356.2 m/z with fragment masses (Q3) 266.2, 311.2, 192.2. The Q3 192.2 ion is the differentiating signal between BAIBA and GABA where the signal is intense for BAIBA and very less for GABA and used for BAIBA analysis in muscle CM and serum samples. Performed by Dr. Yukiko Kitase.

Hind limb Unloading

All experimental procedures were approved by the Institutional Animal Care & Use Committees at the University of Missouri Kansas City (Kansas City, MO, USA). 5-month-old male C57BL/6 mice were randomly divided into two groups consisting of a hind limb suspended (HS) group with L-BAIBA (n=6 mice) and a HS group without L-BAIBA (n=6 mice). During the HS protocol hind limbs were suspended off the ground for 14 days via tail ring inserted between caudal vertebrae and attached to the top of the cage. Suspended mice had full range of motion on front limbs and ad libitum access to food and normal water (n=6) or water supplemented with L-BAIBA (n=6). L-BAIBA was dissolved in drinking water at a concentration of 100mg/kg/day and drinking water was replaced freshly each day.

Performed by Dr. Yukiko Kitase.

Ex Vivo Muscle Contractility at Physiological Temperature

Mice were sacrificed by cervical dislocation and the EDL and soleus muscles were removed for contractility analysis as previously described (78). Muscles were immediately placed into a dish containing a physiological buffer solution (118 mM NaCl; 5 mM KCl; 1 mM MgCl₂; 1 mM NaH₂PO₄; 25 mM NaHCO₃; 2.5 mM CaCl₂; pH 7.40) with 10 mM glucose. This solution was continuously aerated with a 95/5% O₂/CO₂ mixture. EDL and soleus muscles were mounted vertically between two stimulating platinum electrodes and proximal and distal tendons were secured to adjustable isometric force transducers and to a fixed support, respectively. The muscles were immersed into 20 ml bathing chambers containing physiological buffer maintained at 37°C by a heated water circulating pump.

PowerLab® Software (ADIInstruments Inc., Colorado Springs, CO, USA) was used to store

and analyze force data. Stimulatory voltage was provided by a S88X dual pulse digital stimulator (Grass Products, West Warwick, RI, USA) (pulse duration, 1 ms; train duration, 500 ms). Muscles were lengthened until a single tetanus stimulation produced maximal force and remained at this optimal muscle length (L_0) for the duration of the experiment.

Equilibration: EDL and soleus muscles were next allowed a 30 minute equilibration period during which time they were stimulated with intercalating high and low frequency pulse-trains spaced every 3 min which corresponded to maximal (T_{max}) and half maximal ($\frac{1}{2} T_{max}$) isometric force, respectively (200/100Hz for EDL; 160/40Hz for soleus). The proposed stimulation protocol aids with the study of the relative contributions of the contractile proteins (T_{max}) and the sarcoplasmic reticulum ($\frac{1}{2} T_{max}$) to contractile function (81).

Force-Frequency Relationship: Following equilibration, the EDL and soleus muscles were stimulated to contract with frequencies ranging from 1-220 Hz with a periodicity of 3 min to generate the force vs. frequency (FF) relationship. *Zero External Calcium:* Following FF, muscles were allowed to contract at T_{max} and $\frac{1}{2} T_{max}$ at which point the physiological buffer in the chambers was changed to one which did not contain Ca^{2+} but instead 0.1 mM EGTA.

Muscles were contracted for 30 min at T_{max} and $\frac{1}{2} T_{max}$ with a rest interval of 3 min in order to assess dependence of muscle contractility on extracellular Ca^{2+} .

Recovery from Zero Calcium: The physiological buffer was then replaced with the buffer containing 2.5 mM Ca^{2+} and muscles were allowed 30 min of contractions at T_{max} and $\frac{1}{2} T_{max}$ with a periodicity of 3 min.

Fatigue: Next, to induce fatigue, the EDL and soleus muscles were stimulated at T_{max} and $\frac{1}{2} T_{max}$ with a periodicity of 2 seconds for 5 minutes. *Recovery from Fatigue:* Immediately following the fatiguing protocol, the EDL and soleus muscles were allowed 30

min recovery period during which time they were stimulated at T_{max} and $\frac{1}{2} T_{max}$ with a periodicity of 3 min. *Recovery with Caffeine*: The muscles were then allowed a second similar 30 min recovery period with 5mM caffeine added to the chamber bath to gauge overall EC coupling during the recovery period. After the experiment, the L_0 of each muscle was measured and muscles were excised at their myotendonous junctions, blotted dry and weighed. *Force Data*: Muscle force is reported as absolute force (mN). *Slope Data*: The slope of the rising edge of muscle contractions was measured 0-31 ms after the start of the peak. *Tau Data*: Tau was calculated from 90%-0% of peak height during the relaxation phase of muscle contractions. All data is presented as mean \pm SEM.

Ex Vivo Microcomputed Tomography (μ CT)

Right leg tibiae were dissected and fixed for 1 day in 4% paraformaldehyde, and then kept in 70% ethanol at 4°C until use. Specimens were scanned at 55 kV, 145 μ A, high resolution, 10.5 mm voxel, 200 ms integration time. Three-dimensional images reconstructed within the range of 1 mm from the most proximal metaphysis of tibiae were analyzed. Trabecular morphometry was studied by excluding the cortical bone from the endocortical borders using hand drawn contours followed by thresholding, and was characterized with bone volume fraction (BV/TV). Performed by Dr. Yukiko Kitase.

MBTPS1 Study

Dmp1-cre Mbtps1 cKO Mice

Animals were maintained in the University of Missouri-Kansas City Laboratory Animal Research Center under an approved protocol. *Mbtps1*-floxed mice were obtained

from Dr. Jay Horton, Southwest Medical School and Dr. Linda Sandell, Washington University (82); Dmp1-cre mice were obtained from Dr. Lynda Bonewald, University of Missouri-Kansas City (83). Males (*Mbtps1* *flx/+*):*Dmp1*(*cre/+*)) were crossed with females (*Mbtps1*(*flx/flx*)) to obtain *Mbtps1*^{cKO} mice (*Mbtps1*(*flx/flx*):*Dmp1*(*cre/+*)) offspring; this strategy deletes exon 2 of the *Mbtps1* gene and should be effective in ablating expression of all expressed forms containing the catalytic site. Only male *Mbtps1* cKO (*Mbtps1*(*flx/flx*) × *Dmp1*-*cre*(+/-)) and control mice (*Mbtps1*(*flx/flx*)) were used here to limit the study size and the effects of the estrous cycle. Mice were maintained on standard mouse chow with free access to food and water and housed in ventilated cages with filter bonnets in rooms with a regulated 12-h light and 12-h dark cycle. Offspring were found to be viable throughout the pregnancy and postnatal period. Phenotypic characteristics for 12-week-old, and 40-week-old mice were based on observations of *Mbtps1* cKO mice along with a comparable number of control littermates.

***Ex Vivo* Muscle Contractility at Room Temperature**

Mice were sacrificed by cervical dislocation and the EDL and soleus muscles were removed for contractility analysis as previously described (78). Muscles were immediately placed into a dish containing a physiological buffer solution (142 mM NaCl; 5 mM KCl; 1.8 mM MgCl₂; 10 mM HEPES; 2.5 mM CaCl₂; pH 7.40) with 10 mM glucose, continuously aerated with 100% O₂. EDL and soleus muscles were mounted vertically between two stimulating platinum electrodes and proximal and distal tendons were secured to adjustable isometric force transducers and to a fixed support, respectively. The muscles were immersed into 20 ml bathing chambers containing physiological buffer and

experiments were performed at room temperature. PowerLab® Software (ADInstruments Inc., Colorado Springs, CO, USA) was used to store and analyze force data. Stimulatory voltage was provided by a S88 dual pulse digital stimulator (Grass Products, West Warwick, RI, USA) (pulse duration, 1 ms; train duration, 500 ms). Muscles were first lengthened until a single tetanus stimulation produced maximal force and muscles remained at this optimal length (L_0) for the duration of the experiment. *Equilibration:* EDL and soleus muscles were next allowed a 30 minute equilibration period during which time they were stimulated with high frequency pulse trains which corresponded to maximal (T_{max}) isometric force. *Force-Frequency Relationship:* Following equilibration, the EDL and soleus muscles were stimulated to contract with frequencies ranging from 1-130 Hz with a periodicity of 1 min to generate the force vs. frequency (FF) relationship. *Zero External Calcium:* Following FF, muscles were allowed to contract at T_{max} to ensure that the preparation was stable at which point the physiological buffer in the chambers was changed to one which did not contain Ca^{2+} but instead 0.1 mM EGTA. Muscles were contracted for 20 min at T_{max} with an interval of 1 min in order to assess dependence of muscle contractility on extracellular Ca^{2+} . *Recovery from Zero Calcium:* The physiological buffer was then replaced with the buffer containing 2.5 mM Ca^{2+} and muscles were allowed 30 min of contractions at T_{max} with a periodicity of 1 min. *Fatigue:* Next, to induce fatigue, the EDL and soleus muscles were stimulated with at T_{max} with a periodicity of 1 second for 5 minutes. *Recovery from Fatigue:* Immediately following the fatiguing protocol, the EDL and soleus muscles were allowed 30 min recovery period during which time they were stimulated at T_{max} with a periodicity of 1 min. *Recovery with Caffeine:* The muscles were then allowed a second

similar 30 min recovery period with 5mM caffeine added to the chamber bath to gauge overall EC coupling during the recovery period. After the experiment, the L_0 of each muscle was measured and muscles were excised at their myotendonous junctions, blotted dry and weighed. *Force Data:* Muscle force is reported as absolute force (mN) and force normalized to muscle physiological cross sectional area (N/cm^2) as previously reported (78). All data is presented as mean \pm SEM.

Immunohistochemistry of Muscle Cryosections

Soleus muscles and extensor digitorum longus muscles (EDL) were dissected immediately after sacrifice and flash frozen in optimum cutting temperature medium for storage. Muscles were cut into 14- μm -thick sections using a cryostat and then processed for immunofluorescence staining using a protocol adapted from that published by Phillips et al. (84). Briefly, sections were air-dried, acetone-fixed, and then blocked with mouse M.O.M. IgG blocking reagent (Vector Laboratories, Inc.) for 1 h at room temperature. After washing in PBS, sections were incubated overnight in the following mixture of primary antibodies dissolved in PBS containing 2% normal goat serum: 1:100 anti-type I myosin heavy chain (BS.D5 IgG2b, Developmental Studies Hybridoma Bank), 1:200 anti-type IIA myosin heavy chain (SC.71 IgG1, Developmental Studies Hybridoma Bank), and 1:100 anti-type IIB myosin heavy chain (BF.F3 IgM, Developmental Studies Hybridoma Bank). After washing in PBS, sections were treated for 2 h with the following mixture of secondary antibodies dissolved in PBS containing 2% normal goat serum: Alexa Fluor 647-conjugated goat anti-mouse IgG2b (Invitrogen), Alexa Fluor 488-conjugated goat anti-mouse IgG1 (Invitrogen), and Alexa Fluor 594-conjugated goat anti-mouse IgM (Invitrogen). After

washing extensively with PBS, sections were post-fixed in methanol for 5 min, rinsed in PBS, and then cover-slipped with mounting medium including DAPI (Vector Laboratories, Inc.). Sections were imaged using an inverted Nikon TE2000-E epifluorescence microscope and Metamorph software. ImageJ software was used to overlay different colored images of the same field, and then contrast and brightness were adjusted in Photoshop. Performed by Dr. Jeffery Gorski.

Muscle RNA Isolation and Processing for Whole Genome Array

Total RNA was isolated from flash frozen cKO and control soleus muscle samples (n=3 mice per group) using an RNeasy Micro kit according to standard protocols along with the inclusion of a proteinase K digestion step. The RNA was analyzed for quality using a Nanodrop and an Agilent Bioanalyzer after which 100 ng of total RNA were used for the Agilent Mouse Transcriptome Array 1.0 protocol. Briefly, the total RNA was primed with primers containing a T7 promoter sequence. Single-stranded cDNA was synthesized with a T7 promoter sequence at the 5'-end, converted to double-stranded cDNA, and *in vitro* transcribed with T7 RNA polymerase to generate antisense RNA. The cRNA was cleaned up using a bead protocol and then used to synthesize sense strand cDNA in a reaction that included dUTP at a fixed ratio relative to dTTP. RNase H was used to hydrolyze the cRNA strand after which the sense strand cDNA was purified using beads and then fragmented at the unnatural dUTP residues using uracil-DNA glycosylase and apurinic/apyrimidinic endonuclease 1. The fragmented cDNA was labeled by terminal deoxynucleotidyltransferase using the Affymetrix proprietary DNA Labeling Reagent that is covalently linked to biotin. The biotinylated and fragmented cDNA was hybridized

overnight to the Mouse Transcriptome 1.0 arrays after which it was washed and stained on a FS450 GeneChip system and scanned using a GCS30007G scanner.

The CEL files from muscle or bone osteocytes then were analyzed using Affymetrix Expression Console and Transcriptome Analysis Console 2.0. For detailed statistical analysis, the CEL files were imported into GeneSpring v13, quantile-normalized using the PLIER16 algorithm, and baseline-transformed to the median of all samples. The log₂-normalized signal values were then filtered to remove entities that showed signal in the bottom 20th percentile across all samples. The above lists were subjected to a t test ($P < 0.05$) with a Benjamini-Hochberg false discovery rate correction. Performed by Dr. Jeffery Gorski.

Statistics

Data was statistically analyzed with either two-tailed independent samples t-test for single comparisons or with one-way ANOVA followed by Tukey for multiple comparisons with $p < 0.05$ considered the threshold for significance. Normality of the data was assessed with Shapiro-Wilks test and homogeneity of variances was determined using Levene's test.

CHAPTER 3

RESULTS

BAIBA Study

L-BAIBA but Not D-BAIBA is Released from Isolated Contracting Skeletal Muscles

In order to directly measure isomeric composition of BAIBA released from skeletal muscles during contractile activity we choose to isolate whole intact slow-twitch (soleus) and fast-twitch (EDL) skeletal muscle groups from healthy adult mice for the generation of conditioned media through an established *ex vivo* muscle contraction protocol (Illustration 1). As the neuronal components required for contraction are removed from the muscles during the dissection process we can directly manipulate muscle contractile output in this setup through controlled supply of electrical stimulation. We detected an approximately 5-fold increase in the concentration of BAIBA in the MCM from actively contracting muscles relative to inactive/static muscle preparations ($P<0.05$) (Illustration 2). Additionally, LC/MS analysis of the preferred isomeric state of muscle-released BAIBA revealed that the L-form and not the D-form of BAIBA is exclusively jettisoned from skeletal muscle during *ex vivo* contraction (Illustration 2). We did not detect any statistical difference ($P>0.05$) in BAIBA release properties between the chosen representative slow-twitch soleus and fast-twitch EDL muscles or among males and females (Illustration 2).

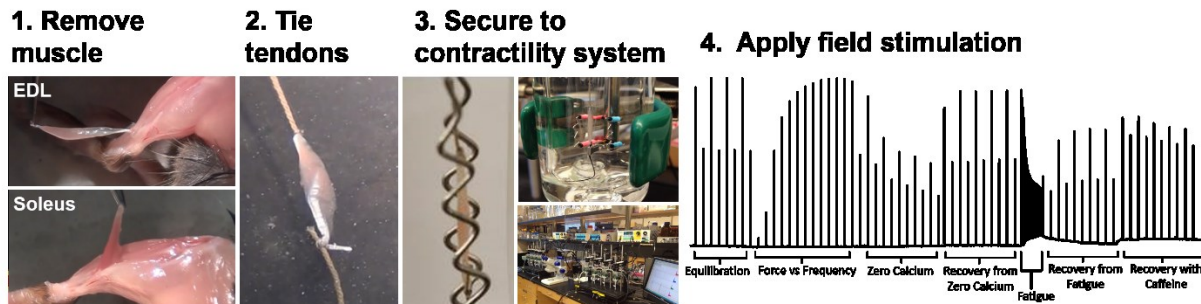


Illustration 1. *Ex vivo* Contractility Methodology. Left: Photographs showing protocol for EDL and soleus muscle dissection and mounting to the *ex vivo* contractility system for contractile force measurements. Right: Representative raw force data from an entire contractility assay.

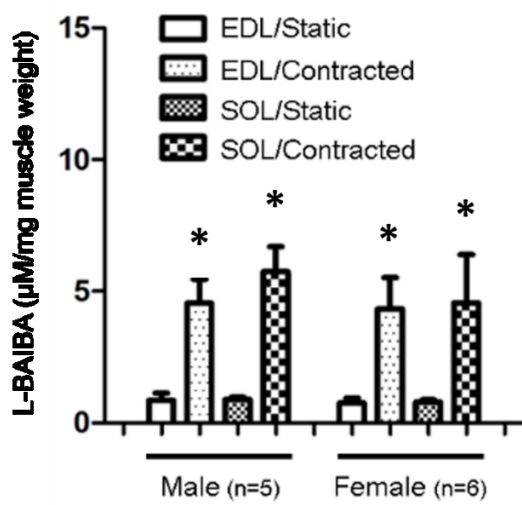


Illustration 2. LC/MS Quantification of L-BAIBA in MCM. L-BAIBA was quantified in MCM by LC/MS from static (non-contracted) or contracted EDL and soleus muscles isolated from hind limbs of wild type, 5-month-old C57BL6 mice. *P<0.05 vs corresponding non-contracted muscle. Data provided by Dr. Yukiko Kitase.

L-BAIBA Supplementation Maintains Contractile Force in Soleus Muscles During Unloading

Based on the LC/MS analysis of secreted BAIBA isomers from muscle we supplemented mice with 100mg/kg/day of L-BAIBA during a 2 week bout of hind limb unloading to probe for a potential therapeutic utility in protecting against muscle structural and functional deterioration during sustained disuse. EDL and soleus muscles were dissected from L-BAIBA supplemented and non-supplemented mice after the unloading period for *ex vivo* contractility testing and morphometric analysis. Included in the contractility analysis were 6 mice per group, with 12 EDL muscles and 12 soleus muscles analyzed per group (muscles from both hind limbs per mouse were tested). Representative data from a contractility experiment are shown in Illustration 1. At the end of 14 days of hind limb unloading, soleus muscle morphometric properties including wet weight and optimal length showed no differences across the control and L-BAIBA treated groups (Illustration 3A-B, P>0.05, n=6 mice per group). Analysis of the force-frequency relationship in the isolated muscles showed no relative shifts in the relative soleus muscle frequency-dependent force production among groups (Illustration 3C). Evaluation of isometric force production from L-BAIBA supplemented muscles revealed a 15% increase in soleus muscle submaximal force generation (40 Hz stimulation frequency, corresponding to approx. half of the maximal force generating capacity ($\frac{1}{2} T_{max}$)), (80.1 mN \pm 3.0 mN vs. 69.7 mN \pm 3.6 mN, P<0.05, n=6 mice per group) while maximal force generation was not significantly altered compared to soleus muscles from control mice (Illustration 3D-E). We next analyzed kinetic properties of individual muscle submaximal and maximal contractions

including the rate of force development of the muscle contraction (dF/dt) and rate of relaxation (Tau). The rate, or slope, of force development at $\frac{1}{2} T_{max}$ in the soleus muscles from the L-BAIBA supplemented group was significantly elevated by 16% compared to control ($0.309 \text{ mN/ms} \pm 0.014 \text{ mN/ms}$ vs $0.267 \text{ mN/ms} \pm 0.011 \text{ mN/ms}$, $P<0.05$, $n=6$ mice per group) (Illustration 3F-G). The rate of submaximal and maximal force relaxation was similar among soleus (Illustration 3H-I) muscles from supplemented and non-supplemented groups. On the other hand, no statistically significant effects of L-BAIBA supplementation were found in the EDL muscles with regard to muscle size and contractile force properties (Illustration 4A-H).

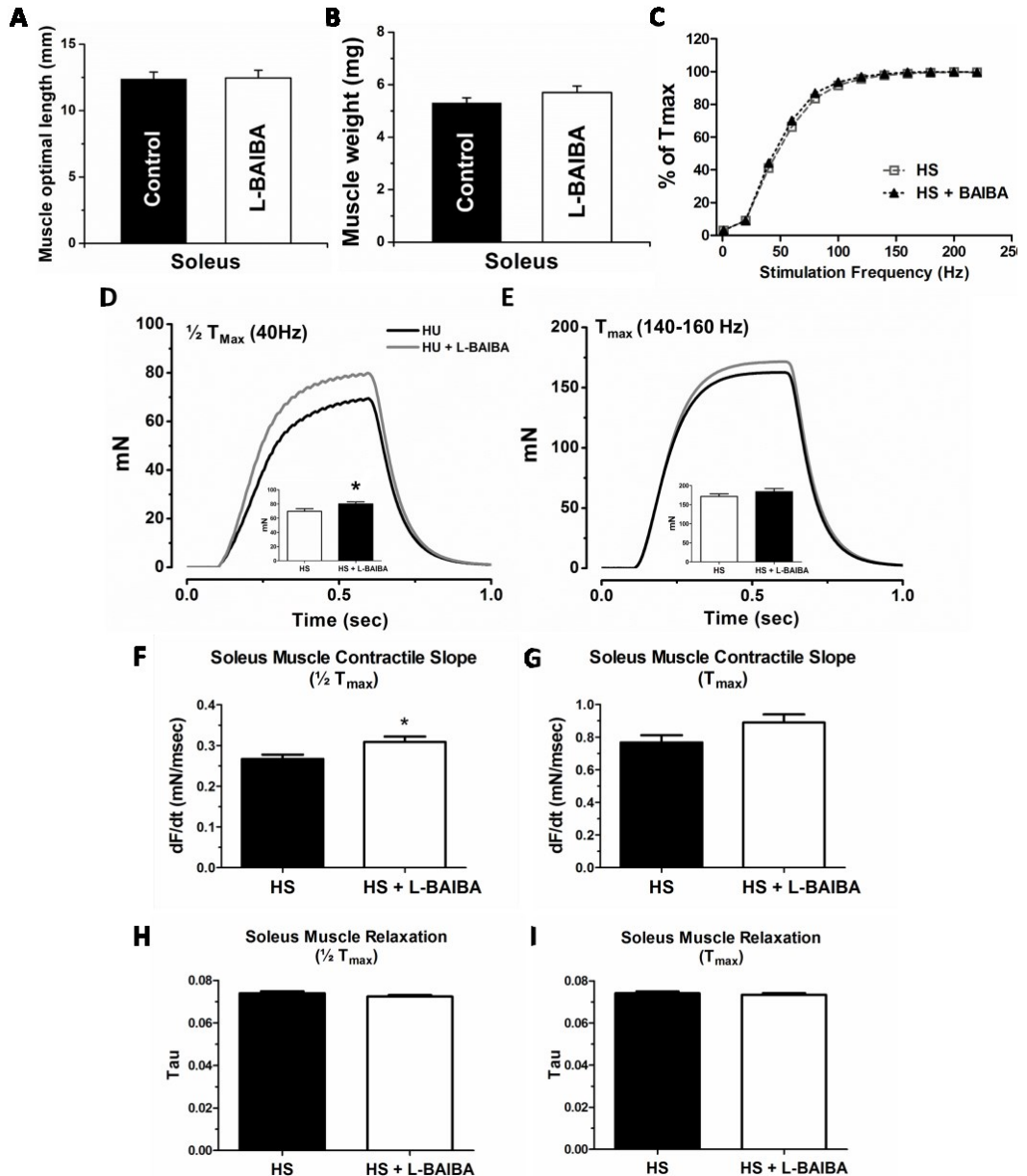


Illustration 3. Ex Vivo Contractility of Hind Limb Suspended Soleus Muscle. A) Soleus muscle optimal length. B) Soleus muscle mass. C) Force-frequency relationship of soleus muscle stimulated with frequencies ranging from 1-220Hz. D) Raw data trace of soleus muscle 1/2 Tmax contraction (40Hz) and bar graph comparison (inset) from L-BAIBA and control groups. E) Raw data trace of soleus muscle Tmax contraction (140-160Hz) and bar graph comparison (inset) between groups. F) Slope of soleus muscle 1/2 Tmax contraction (40Hz). G) Slope of soleus muscle Tmax contraction (140-160Hz). H) Soleus muscle relaxation (Tau) of 1/2 Tmax contraction (40Hz). I) Soleus muscle relaxation (Tau) of Tmax contraction. N=6 mice per group, * denotes p<0.05 versus control group.

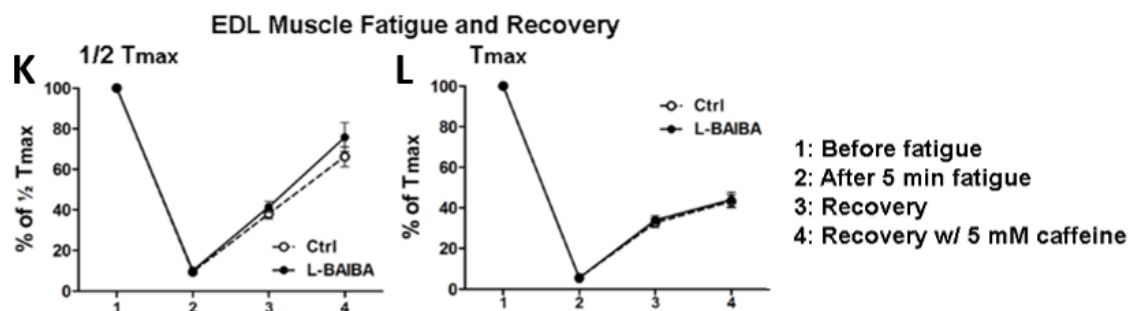
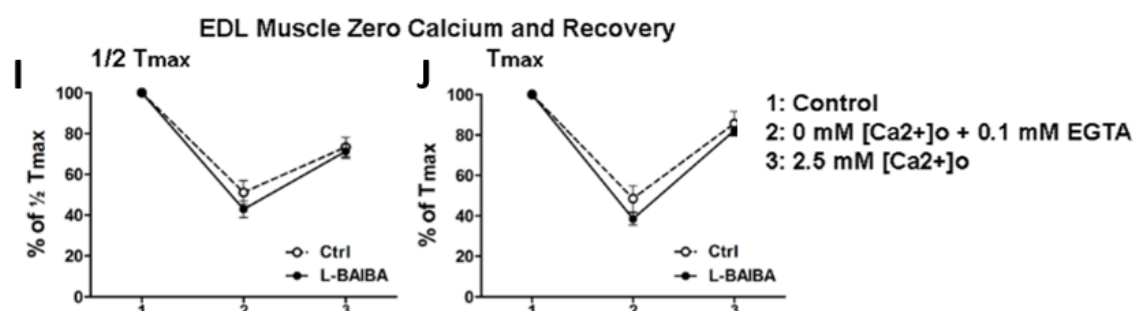
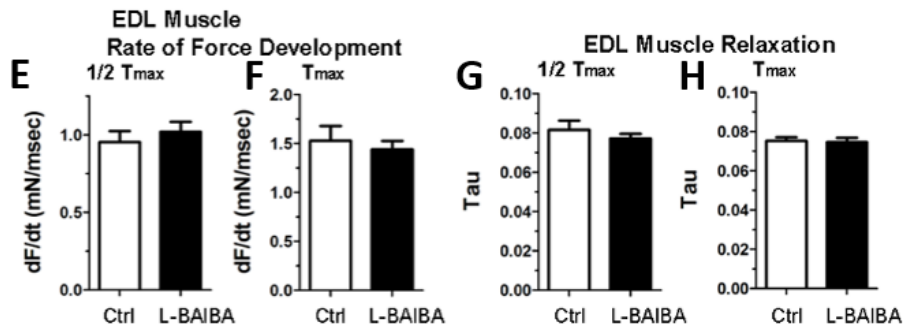
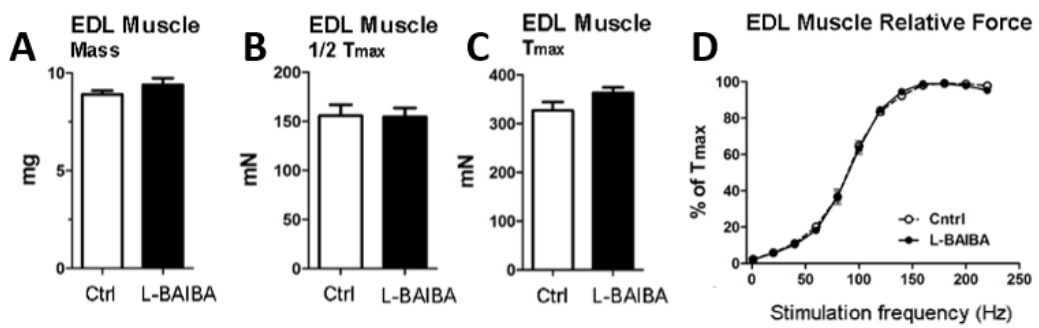


Illustration 4. Ex Vivo Contractility of Hind Limb Suspended EDL Muscle. A) EDL muscle mass. B) EDL muscle 1/2 Tmax (100Hz stimulation frequency). C) EDL muscle Tmax (200Hz stimulation frequency). D) Force-frequency relationship of EDL muscle stimulated with frequencies ranging from 1-220Hz. E) Slope of EDL muscle 1/2 Tmax contraction. F) Slope of EDL muscle Tmax contraction. G) EDL muscle relaxation (τ) of 1/2 Tmax. H) EDL muscle relaxation (τ) of Tmax. I) EDL muscle force generation after replacement of bathing solution with solution devoid of Ca^{2+} and instead containing 0.1 mM EGTA and after reintroduction of 2.5 mM Ca^{2+} at Tmax and (J) 1/2 Tmax. Data is expressed as a percentage of force just prior to removal of external calcium. K) EDL muscle fatigueability, recovery from fatigue and response to 5mM caffeine at Tmax and (L) 1/2 Tmax. Expressed as a percentage of force just before fatigue. N=6 mice per group.

L-BAIBA Does Not Affect Muscle Dependence on Extracellular Ca^{2+} or Fatigue/Recovery from Fatigue

We also investigated the dependence on extracellular calcium and fatigue resistance and recovery from fatiguing contractions in both EDL and soleus muscles. Maximal and submaximal force generation from L-BAIBA supplemented and non-treated suspended muscles showed indistinguishable force production profiles upon depletion of external calcium and after reintroduction of 2.5 mM calcium to the bathing buffer (Illustration 4I-J and 5A-B). It has been shown that hind limb unloading in mice results in deficiencies to muscle fatigue resistance and force recovery following muscle fatigue (19). Muscle fatigueability at maximal or submaximal force and recovery after fatigue in the absence and presence of caffeine, which effectively releases calcium from the sarcoplasmic reticulum (SR), showed no significant difference between groups (Illustration 4K-L and 5C-D).

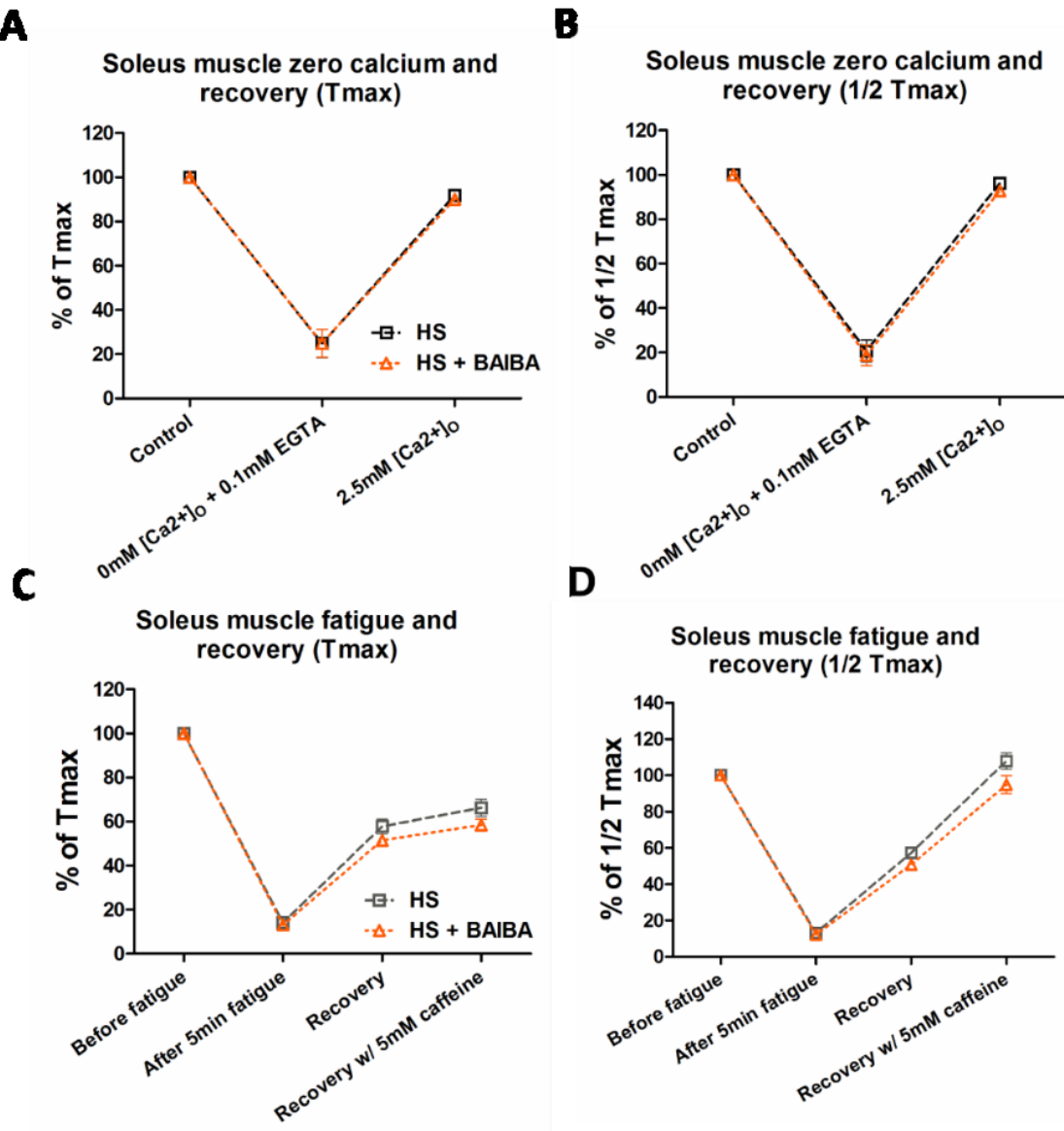


Illustration 5. Soleus Muscle Dependence on External Ca²⁺ and Fatigue/Recovery

Properties. Soleus muscle force generation after replacement of bathing solution with solution devoid of Ca²⁺ and instead containing 0.1 mM EGTA and after reintroduction of 2.5 mM Ca²⁺ at Tmax (A) and 1/2 Tmax (B). Data is expressed as a percentage of force just prior to removal of external calcium. Soleus muscle fatigueability, recovery from fatigue and response to 5mM caffeine at Tmax (C) and 1/2 Tmax (D) expressed as a percentage of force just before fatigue. N=6 mice per group.

Preserved Tibial Trabecular Bone Volume in Mice Supplemented With L-BAIBA

A hallmark of the removal of weight bearing load on skeletal bone is a marked reduction in trabecular bone volume fraction (BV/TV) which is associated with compromised bone structural integrity (85). In a study performed in parallel with the muscle function characterization, we measured trabecular bone content in L-BAIBA supplemented and control mice through analysis of BV/TV in whole tibiae via *ex vivo* μ CT imaging. We found that trabecular BV/TV was statistically significantly increased in the tibiae from the L-BAIBA treated group over control group (Illustration 6) indicating that bone loss was spared with L-BAIBA treatment during hind limb unloading.

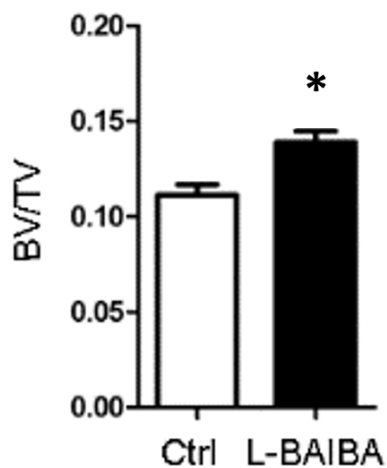


Illustration 6. Bone Content of Hind Limb Suspended Mice. Trabecular bone volume fraction (BV/TV) of right side tibiae from mice treated with L-BAIBA or non-treated mice after 2 weeks of hind limb unloading as determined by *ex vivo* μ CT. *P<0.05 vs control mice. Data provided by Dr. Yukiko Kitase

MBTPS1 Study

Soleus Muscles but Not EDL Muscles from Adult *Mbtsp1* cKO Mice Are Larger and Produce More Contractile Force

We assessed the size and *ex vivo* contractile properties of isolated EDL and soleus muscle from 10 month old *Mbtsp1* cKO mice and age matched control littermates. A representative image of the *ex vivo* contractility protocol is shown in Illustration 7A. Soleus muscles from *Mbtsp1* cKO mice but not EDL muscles were larger than muscles from control animals ($10.5 \text{ mg} \pm 0.4 \text{ mg}$ vs $9.3 \text{ mg} \pm 0.4 \text{ mg}$, $P<0.05$, $n=5$ mice per group) (Illustration 7B). Not only were the soleus muscles larger in the cKO, but they displayed a 30% increase in absolute contractile force and force normalized to muscle physiological CSA ($P<0.05$) (Illustration 7C-E). Interestingly, when similar contractile characterization was carried out on EDL muscles, there were no significant differences observed between *Mbtsp1* cKO and control mice ($P>0.05$) (Illustration 7F-G).

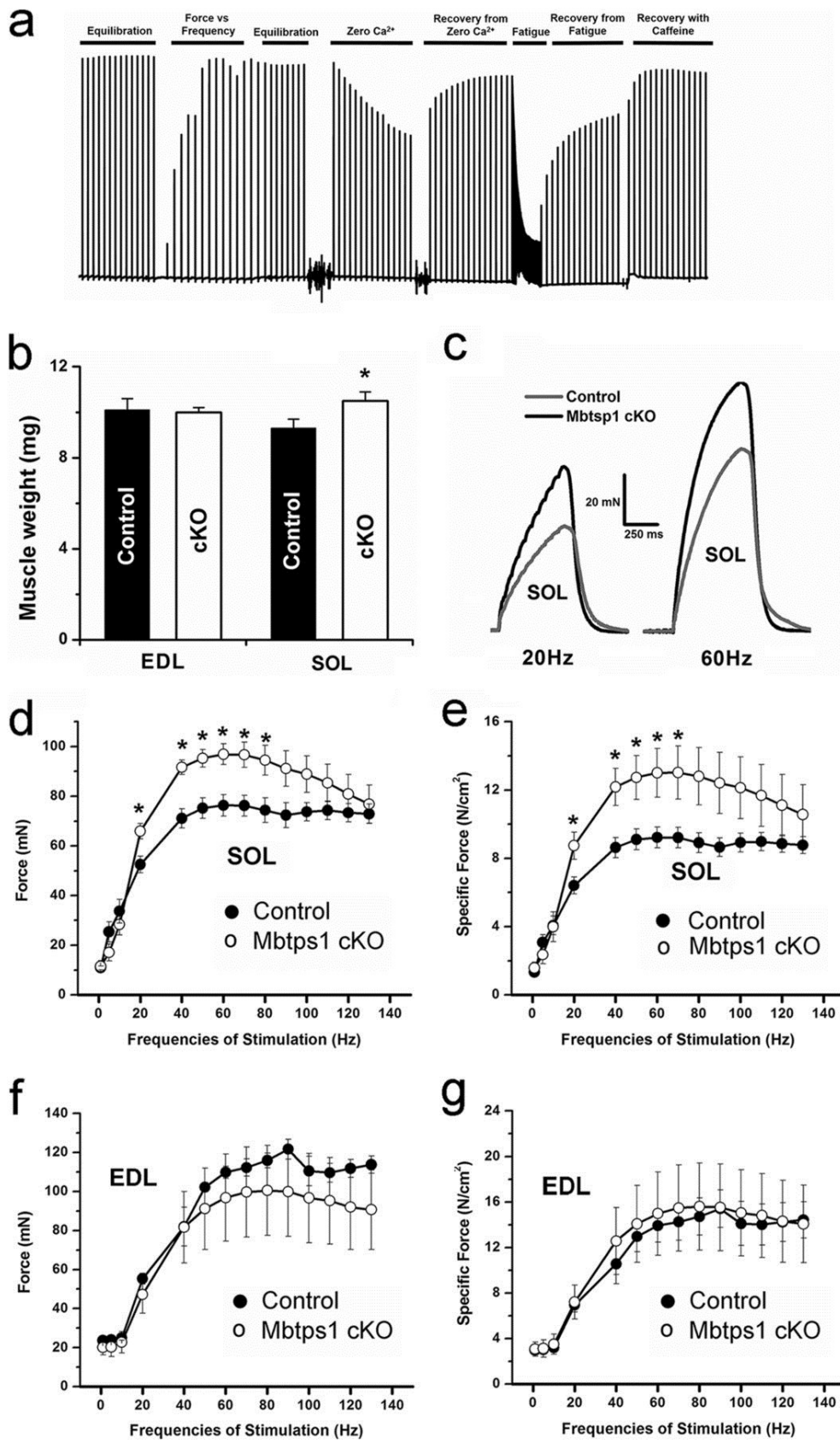


Illustration 7. Muscle Size and Contractile Force of 10 Month-Old *Mbtps1* cKO Mice. a) Representative data obtained from individual muscles during the *ex vivo* contractility assay. Intact EDL and soleus muscles were mounted between two platinum electrodes and stimulated with non-tetanic and tetanic voltage trains to induce muscle contraction (y axis, contractile force; x axis, time.) b) EDL and soleus muscle mass from control and *Mbtps1* cKO mice. c) Individual contractions of submaximal (left) and maximal (right) tetanic contractions of intact soleus muscles from control (grey line) and *Mbtps1* cKO (black line) mice stimulated *ex vivo*. d) soleus muscle absolute contractile force from control mice and *Mbtps1* cKO mice at increasing frequencies of stimulation in the range of 1–130 Hz. e) soleus muscle contractile forces from d normalized to cross-sectional area of the muscle (newtons (N)/cm²). f) Absolute contractile force (millinewtons) of intact EDL muscles from control and *Mbtps1* cKO mice stimulated at frequencies of 1–130 Hz. g) EDL muscle forces from f normalized to muscle cross-sectional area (newtons/cm²). Data are represented as mean ± SEM. * denotes significant difference ($P < 0.05$) when compared with control, n=5 mice per group.

Soleus Muscles from Adult *Mbtps1* cKO Mice Display Rightward Shift of the Force-Frequency Relationship

The force-frequency relationship of soleus muscles from 10 month old adult *Mbtps1* cKO mice showed a significant shift to the right at several submaximal frequencies of stimulation ($P < 0.05$, n=5 mice per group) (Illustration 8A). This shift indicated that higher frequencies of stimulation were required in soleus from the *Mbtps1* cKO to elicit the same amount of contractile force in the soleus muscle from control littermates. Soleus muscle fatigue, recovery from fatigue and caffeine response properties were not statistically different among cKO and control groups (Illustration 8B). We also examined the effect of removal and subsequent reintroduction of calcium to the bathing buffer on force production and observed a similar response between groups (Illustration 8C). The EDL muscles from *Mbtps1* cKO mice did not display any shifts in the force-frequency relationship or differences in fatigueability/recovery post fatigue or response to removal and re-addition of extracellular calcium to the bathing solution (Illustration 8D-F).

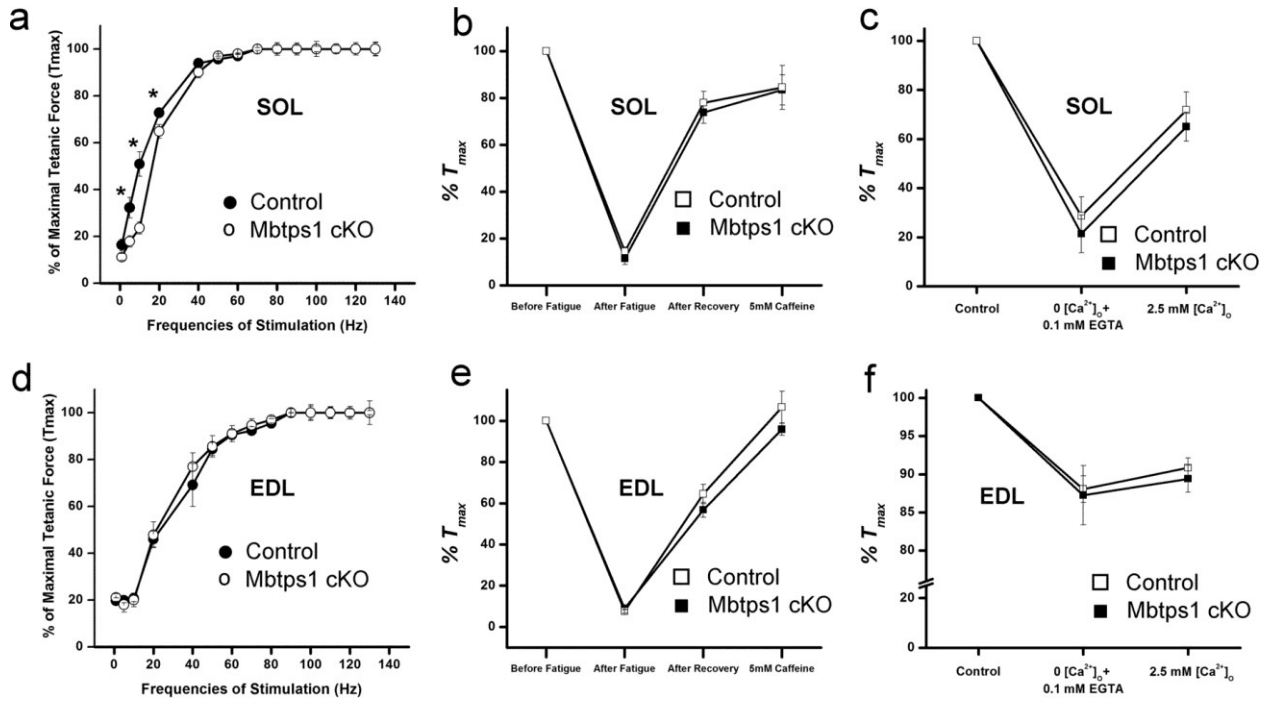


Illustration 7. Contractile Properties of 10 Month-Old *Mbtps1* cKO Mice. a) Force versus frequency relationship of soleus muscles from control and *Mbtps1* cKO mice stimulated with frequencies ranging from 1 to 130 Hz. Force is expressed as a percentage of maximum muscle force (T_{max}). b) Fatigueability of soleus muscles from control and *Mbtps1* mice and recovery of force during a period of non-fatiguing tetanic stimulations in both the absence and presence of 5 mM caffeine. Data are expressed as a percentage of force produced by the muscle prior to fatigue. c) Dependence on external calcium for force production of soleus muscles from control and *Mbtps1* cKO mice contracted under external conditions of 0 $[Ca^{2+}]_o$ and after replenishment of 2.5 mM $[Ca^{2+}]_o$ for force recovery. Data are expressed as a percentage of force produced by the muscle prior to removal of $[Ca^{2+}]_o$. d) EDL muscle force versus frequency (1–130 Hz) relationship from control and *Mbtps1* cKO mice. Force is expressed as a percentage of maximum muscle force (T_{max}). e) Fatigueability of EDL muscle from control and *Mbtps1* mice and force recovery after a period of non-fatiguing tetanic stimulations in both the absence and presence of 5 mM caffeine. Data are expressed as a percentage of force produced by the muscle prior to fatigue. f) Dependence on external calcium for force production of EDL muscle from control and *Mbtps1* mice contracted in external conditions of 0 $[Ca^{2+}]_o$ and after washout with 2.5 mM $[Ca^{2+}]_o$ for force recovery. Data are expressed as a percentage of force produced by the muscle prior to removal of $[Ca^{2+}]_o$. Data are represented as mean \pm SEM. * denotes significant difference ($p < 0.05$) when compared with control, $n=5$ mice per group.

Type 1 Myosin Heavy Chain-Expressing cKO Soleus Muscle Myofibers Exhibit Centralized Nuclei

In order to investigate phenotypic changes at the myofiber level, immunohistochemistry was carried out on cryosections of soleus muscles from 10 month old *Mbtps1* cKO and control mice. DAPI staining (yellow) revealed a 700% increase in the amount of centralized nuclei within cKO myofibers compared to control, a characteristic of active muscle generation ($21.5\% \pm 5.7\%$ vs $3.5\% \pm 2.9\%$, mean \pm SD, $P<0.05$.) (Illustration 9). Furthermore, muscle cross sections were fiber-typed through immunostaining for specific MHC type 1 and type 2 isoforms. Fiber-typing showed that the central nuclei phenotype within cKO soleus muscles occurred specifically in MHC type 1 expressing myofibers while neighbouring MHC type 2-containing cells were unaffected and exhibited normal levels of central nuclei (Illustration 9). Conversely, EDL muscle cryosections were indistinguishable among cKO and control with respect to centralized nuclei content (Data not shown).

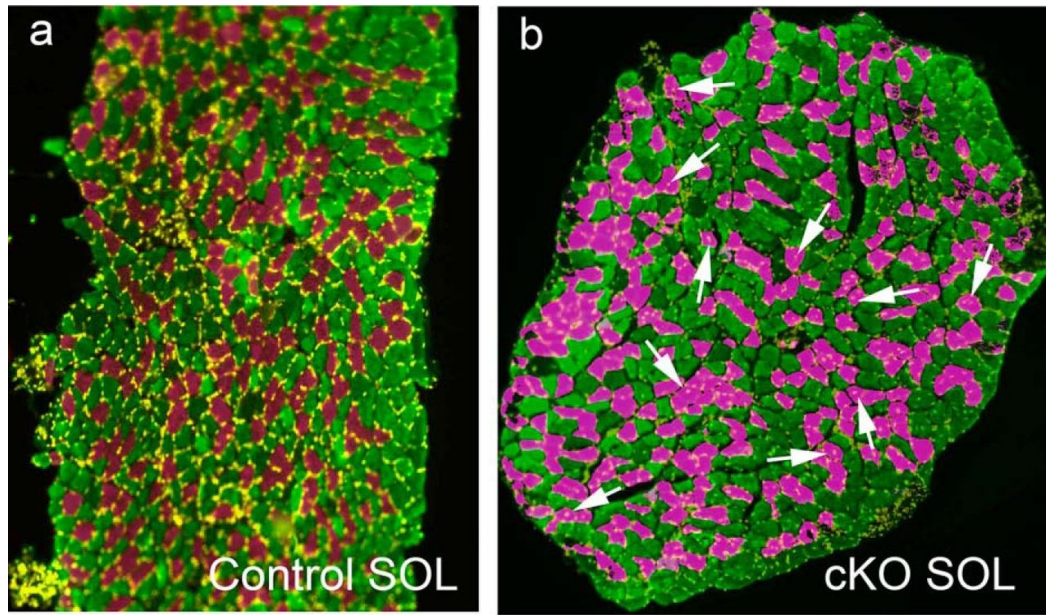


Illustration 9. Immunostaining of Soleus Cryosections. Muscles from adult Dmp1-cre *Mbtps1* cKO and control mice were dissected immediately following euthanasia and flash frozen, cryosectioned and immunostained as described under “Experimental Procedures.” Images of whole muscle cross-sections were pseudocolored using ImageJ. Magenta-colored myofibers: cKO soleus muscle is enriched in type 1 myosin heavy chain-expressing cells (magenta-colored myofibers) with centralized nuclei (white arrows), whereas type 1 myosin heavy chain-positive and type IIA heavy chain-positive (green-colored myofibers) control cells contain only background levels of centralized nuclei. Nuclei were identified by DAPI staining (yellow color). a) Control soleus muscle; b) Dmp1-cre *Mbtps1* cKO muscle. Images shown were photographed at 10x magnification. Data provided by Dr. Jeff Gorski.

Contractile Properties of Soleus and EDL Muscles from 3-Month Old *Mbtps1* cKO Mice

Mbtps1 cKO mice show an increase in body mass occurring abruptly at around 15-20 weeks of age that persists throughout maturation (data not shown). In order to determine if the phenotypic changes observed in the soleus muscles of 10-12 month old *Mbtps1* cKO mice was related to changes observed in body mass, we performed contractility analysis on isolated EDL and soleus muscles from young cKO mice aged to 3 months, which is just prior to the point at which cKO begin to accumulate body mass.

Unlike their mature adult counterparts, young cKO soleus muscle mass, contractile strength, and force-frequency response was not significantly different compared to control mice (Illustration 10A-B, D-E). Examination of muscle fatigue and recovery also showed no change in soleus or EDL muscles among cKO and control groups. Interestingly, EDL muscles from young cKO mice produced about 25% more specific force normalized to muscle CSA than controls which was not detected in EDL muscles from the mature adult *Mbtsp1* cKO mice (Illustration 10H, P<0.05, n=5 mice per group).

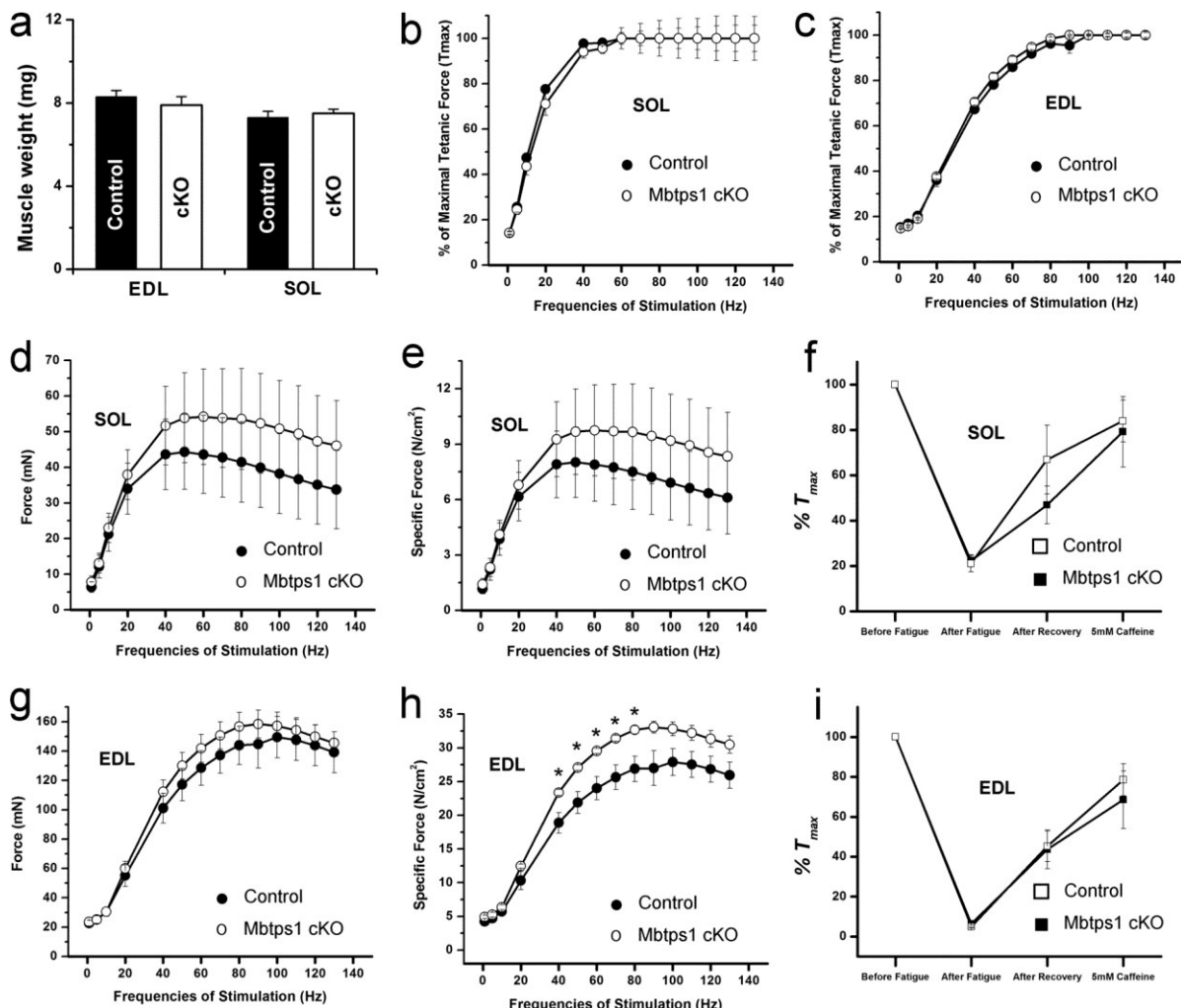


Illustration 10. Contractile Properties of 3 Month-Old *Mbtps1* cKO Mice. a) EDL and soleus muscle wet weights from control and *Mbtps1* cKO mice. b) Force versus frequency curves of intact soleus muscles from control and *Mbtps1* cKO mice stimulated at individual frequencies ranging from 1 to 130 Hz. Force is normalized to maximum muscle force (T_{max}) and expressed as a percentage. c) EDL muscle force versus frequency (1–130 Hz) curves from control and *Mbtps1* cKO mice. Contraction force is normalized to T_{max} of the muscle and expressed as a percentage. d) Soleus muscle contractile force (millinewtons (mN)) from control mice and *Mbtps1* cKO mice at increasing frequencies of stimulation in the range of 1–130 Hz. e) Soleus muscle contractile forces from d normalized to cross-sectional area of the muscle (newtons (N)/cm²). f) Relative contractile force of soleus muscles from control and *Mbtps1* cKO mice after a fatigue-inducing stimulation protocol and after a recovery period of non-fatiguing tetanic stimulations in both the absence and presence of 5 mm caffeine. Data are expressed as a percentage of force produced by the muscle prior to fatigue. g) Contractile force (millinewtons) of intact EDL muscles from control and *Mbtps1* cKO mice stimulated at frequencies of 1–130 Hz. h) EDL muscle forces from g normalized to muscle cross-sectional area (newtons/cm²). i) EDL muscle relative contractile force from control and *Mbtps1* cKO mice after a fatigue-inducing stimulation protocol and after a recovery period of non-fatiguing tetanic stimulations in both the absence and presence of 5 mm caffeine. Data are represented as mean \pm SEM. * denotes significant difference ($p < 0.05$) when compared with control, n=6 control mice and n=4 cKO mice.

Whole Genome Array of cKO Soleus Muscles Provides Clues for Increased Performance

To identify possible candidate mechanisms responsible for augmented cKO soleus muscle performance and morphometric measures we performed whole genome arrays on soleus muscles isolated from 10-month old cKO and control mice (NCBI accession number GSE69985). cKO soleus muscles exhibited significant alterations in expression patterns of various genes involved with muscle contraction, oxidative metabolism, and muscle myogenesis and regeneration. Specifically, myofibrillar and sacromeric genes involved in muscle contraction were upregulated in the cKO including slow-twitch muscle troponin I, the sacro-structural proteins desmin and *Actn2*, and *Syp12*, a gene involved in excitation-contraction coupling (ECC). Additionally, biomarkers of muscle regeneration were induced

in the cKO such as *Myh3* and *Myl4* (embryonic myosin heavy and light chain isoforms) (86, 87). We also detected elevated expression of genes necessary for muscle growth and development such as the myogenic regulatory factor, *Myf6*, the muscle hypertrophic regulator follistatin, and muscle associated receptor tyrosine kinase (*Musk*), which is necessary for neuromuscular junction formation (88). Moreover, changes to glucose and lipid metabolic genes were revealed in cKO muscle including upregulation of muscle glycogen synthase 1 and carnitine acetyltransferase, respectively.

Table 1. Whole Genome Array. Key genes upregulated in soleus muscles from 10 month old *Mbtsp1* cKO and control littermates as assessed for expression by whole genome array. N=3 mice per group. Data provided by Dr. Jeff Gorski.

Gene	Description	Fold change (cKO vs control)	ANOVA p-value (cKO vs. Control)
Actn2	actinin alpha 2	1.14	0.02035
Crat	carnitine acetyltransferase	1.22	0.00709
Des	desmin	1.18	0.01804
Fst	follistatin	1.7	0.02098
Gsk3a	glycogen synthase kinase 3 alpha	1.23	0.03052
Gys1	glycogen synthase 1, muscle	1.3	0.00391
Musk	muscle, skeletal, receptor tyrosine kinase	1.75	0.04724
Myf6	myogenic factor 6	1.59	0.03623
Myh3	myosin, heavy polypeptide 3, embryonic	1.75	0.04934
Myl4	myosin, light polypeptide 4	1.15	0.00097
Sypl2	synaptophysin-like 2	1.41	0.05685
Tnni1	troponin I, skeletal, slow 1	1.21	0.03828

CHAPTER 4

DISCUSSION

Musculoskeletal interaction constitutes a multifaceted and complex interplay involving mechanical coupling as well as bi-directional biochemical signaling through the musculoskeletal secretome, the latter emerging as a new and exciting paradigm of tissue cross-regulation. In the present study we investigated two potential crosstalk pathways within the muscle-bone unit involving the skeletal muscle-derived exercise factor, BAIBA, as well as the role of the bone osteocyte-specific serine protease, MBTPS1, in bone-to-muscle crosstalk. Our results suggest that BAIBA participates in the regulation of bone structure and muscle function as we show that oral supplementation of L-BAIBA reduces bone loss and skeletal muscle contractile decline in a mouse model of extended hind limb disuse. Next, we provide evidence for a novel bone-to-muscle crosstalk pathway involving MBTPS1 since its targeted ablation in osteocytes induced a skeletal muscle regeneration phenotype and enhanced skeletal muscle mass and contractile force output by 10 months of age. Remarkably, the skeletal muscle-specific effects observed in these two crosstalk models were confined to slow-twitch soleus muscles while fast-twitch EDL muscles remained generally unaffected.

The release of BAIBA from skeletal muscle has been demonstrated previously using *in vitro* cell culture as well as serum measures collected post-exercise training (46), however this has not been directly confirmed in fully functional whole muscle samples. Here we show unequivocally that isolated and functionally intact fast and slow-twitch adult skeletal muscles secrete BAIBA in a manner dependent on the onset of muscle contractile

activity. We found that contraction increased muscle-excreted BAIBA ~5 fold compared to uncontracted conditions (Illustration 2). A previous study showed a similar 5.2 fold induction in BAIBA content in gastrocnemius muscle from exercise trained mice (46). We further show by LC/MS isomer profiling that BAIBA is preferentially secreted from skeletal muscle as the L-isomer and that this form displays bioactivity within muscle and bone (Illustration 2). The identification of the preferred isomeric state of muscle-derived BAIBA may indicate that the reported metabolic effects of BAIBA in adipose, liver and skeletal muscle tissues are due to L-BAIBA-specific bioactivity. Thus, specific *in vivo* therapeutic application of L-BAIBA may afford greater potency with regard to impact on health and potential for treating metabolic disorders than the racemic mixture containing both L- and D- isomers.

BAIBA is a known endogenous ligand of mas-related G-protein coupled receptor D (MRGPRD), belonging to the Mas-related gene family of G-protein-coupled receptors (89). MRGPRD is expressed highly in the dorsal root ganglion where it participates in itch/pain neuro-sensation but is also expressed in a number of other tissues including white/brown adipose, brain, testis, lung, gastrointestinal tract, cardiovascular system and skeletal muscle (90). Activation of MRGPRD upon ligand-binding results in a downstream increase in intracellular calcium concentration ($[Ca^{2+}]_i$) via the coupled action of the G-protein alpha subunit, G_q (91). L-BAIBA treatment during hind limb unloading led to enhanced contractile force of the soleus muscle when stimulated at the sub-optimal frequency of stimulation producing about 50% of maximal tetanic force (40 Hz) (Illustration 3). Muscle contractility elicited at high and low frequency impulse stimulation is influenced differently by

intramuscular factors such as Ca^{2+} mobilization, ECC and contractile protein interaction. Low frequency stimulation producing sub-optimal contractile force is highly dependent on alterations to calcium availability and ECC efficiency, whereas in high-frequency maximal force production the activation level is saturated and less prone to changes in ECC (81, 92). Thus, chronic stimulation of MRGPRD through BAIBA supplementation may result in significantly elevated baseline $[\text{Ca}^{2+}]_i$ and increase the free Ca^{2+} available for contractility at sub-maximal frequencies of stimulation. The enhanced rate of force development at the sub-optimal stimulation frequency of 40 Hz (Illustration 3) in L-BAIBA supplemented soleus muscles further supports increased $[\text{Ca}^{2+}]_i$ for activation of contraction. On the other hand we did not detect similar effects in fast-twitch EDL muscle with supplementation (Illustration 4). One possible explanation for these fiber-specific results involves differential fiber-type responsiveness to increased $[\text{Ca}^{2+}]_i$ with slow-twitch fibers from soleus muscle showing a lower calcium-activation threshold for contraction relative to fast-twitch EDL muscle fibers (93). It is also likely that the different metabolisms of fast and slow-twitch muscles played a role in the targeted effects of BAIBA. Slow twitch muscles display preferential oxidative metabolism and abundant mitochondria while fast muscles rely heavily on the glycolytic production of ATP. Mitochondria are a core site for dysfunction during the adaptation of muscle to unloading conditions leading to reduced mitochondrial density, decreased oxidative metabolic gene expression, lower respiratory capacity and redox imbalance. BAIBA has been shown to be an activator of genes involved in fatty acid oxidation which may help to boost mitochondrial function and viability during the myo-adaptive response to disuse. Therefore, the targeted effects of BAIBA on slow-twitch soleus

muscle may be underscored by the intrinsic contractile properties of slow type MHC or the vulnerability of slow-twitch muscle plasticity to disuse.

BAIBA treatment during hind limb unloading resulted in a higher trabecular bone BV/TV value compared to bones from control mice indicating that BAIBA treated animals had a higher bone content (Illustration 5). This effect may be attributed to either suppression of bone resorption and/or stimulation of bone formation by BAIBA. Interestingly, BAIBA has been shown to increase mitochondrial respiration and insulin signaling through AMPK mediated pathway in skeletal muscle (48), adipose (27) and liver (31). In bone, AMPK acts as a negative regulator of osteoclast differentiation by inhibiting RANKL signaling and is therefore a prominent figure in the regulation of bone health and structural homeostasis. Ablation of AMPK catalytic activity within bone resulted in increased remodeling and ultimately bone loss (94). On the other hand, AMPK activation in bone results in an anabolic response (95). Therefore, the bone protective effects of BAIBA are likely mediated through AMPK signaling by suppressing bone loss during hind limb disuse. These findings further supports the existence of an exercise-dependent hormonal pathway in the regulation of bone health involving circulating BAIBA derived from contracting skeletal muscle.

Next, we investigated bone-to-muscle crosstalk. We specifically probed the contribution of the protease MBTPS1 in bone-to-muscle communication and found that deletion of *Mbtsp1* in bone osteocytes resulted in an age-related slow-twitch muscle phenotype involving increased soleus muscle mass and enhanced force generation. We show that this muscle phenomenon is absent in 12-week old (3-month) soleus muscles

(Illustration 10) indicating that the cKO-induced transformation occurs after this developmental time point. Apart from a 25% increase in stiffness (data not shown), bone was essentially unaltered under *Mbtps1* deletion suggesting that a bone-to-muscle endocrine crosstalk mechanism and not altered functional coupling is responsible for the muscle phenotype. Surprisingly, soleus muscles from mature *Mbtps1* cKO mice produced ~30% more contractile force (mN) than control mice (Illustration 7) even when normalized to the size dimensions of the muscle (N/cm²) (Illustration 7). These findings indicate that additional protein and metabolic alterations which are independent of muscle size are contributing to contractile force development in the cKO muscle. Upon evaluation of soleus muscle gene expression profiles by whole genome array we found altered expression of genes related to muscle contraction in the cKO (Table 1), namely in *Actn2*, desmin, *Musk* and *Sypl2* expression. ACTN2 (α -actinin 2) is an actin-binding protein family member and is a major structural component of the Z-disc where it anchors actin-thin filaments and forms contacts with numerous sarcomeric structural proteins including titin and dystrophin aiding in the stabilization of the contractile apparatus during muscle contraction. ACTN2 is normally localized to both type-2 and type-1 muscle fibers (96) and has been found to increase in content inside fast and slow twitch myofibers after both sprint-type training and endurance exercise in mice (97, 98). Desmin is the predominant intermediate filament protein in skeletal muscle and plays a central structural role in sarcomeric scaffolding at the Z-disk as well as anchoring the contractile apparatus to cytoskeletal domains at the sarcolemma (99). Desmin is important for skeletal muscle structural integrity (100), for active and passive force transmission (101, 102) and for proper ECC

(103). *MusK* encodes a muscle specific receptor tyrosine kinase required for proper formation and maintenance of the post-synaptic neuromuscular junction (NMJ) (88). *MusK* becomes highly expressed in differentiating myoblasts during muscle development but becomes substantially downregulated and localized only to NMJ sites in mature adult muscle (104). Inactivating mutations in *MusK* cause congenital myasthenic syndrome which is characterized by severe muscle weakness and increased fatigability due to aberrant ECC from the absence or degradation of NMJs (105). NMJ activation plays an important role in the determination of skeletal muscle fiber type and contractile properties. Soleus muscles cross-innervated with neuronal components normally localized to fast twitch muscles display contractile properties similar to that of fast twitch muscles including elevated force-velocity, faster relaxation and lower relative tension at sub-optimal frequencies of stimulation (106). Interestingly, the latter characteristic was observed in cKO soleus muscles as a rightward-shifted force-frequency curve (Illustration 8) resembling that of a more fast-twitch muscle. Finally, SYPL2 (synaptophysin-like 2) is a synaptophysin protein linked to muscular ECC dysfunction with aging (107). Mice deficient in *Sypl2* display triad junction abnormalities, deficiencies in SR Ca²⁺ uptake and release, reduced force and increased susceptibility to fatigue (108, 109) while upregulation of *Sypl2* is associated with improved muscle function (110). Taken together, the genetic data align with functional properties of cKO slow-twitch soleus muscles to suggest that enhanced structural fortification and force transmission, altered NMJ activity, and improved ECC could be collectively contributing to the functional properties cKO soleus muscle.

Soleus muscles from 10-month old *Mbtps1* cKO mice were larger (Illustration 7) than control. Interestingly, expression of follistatin, which is essential for skeletal muscle development and post-natal muscle hypertrophy (111), was augmented in cKO soleus muscles. Follistatin is a TGF- β antagonist able to bind to and inhibit the actions of myostatin *in vivo* (112) and stimulate mTOR activity (113). Muscles from mice with genetic deletion of follistatin have less mass, reduced contractile force and show compromised regenerative ability after injury (114). Conversely, delivery of follistatin-overexpressing adeno-associated virus vector to skeletal muscle groups causes profound muscle hypertrophy and enhanced strength (113, 115). Thus, repression of TGF- β signaling by follistatin in cKO soleus muscles could be ultimately responsible for the phenotypic changes seen in muscle mass and force. In cKO soleus muscles, we found a 7-fold increase in centralized nuclei exclusively within MHC type-1 expressing fibers (Illustration 9). Myonuclei are normally localized to the periphery and adjacent to the sarcolemma while centralized nuclei are apparent within myofibers during active muscle regeneration (116). Minor muscle damage caused by day to day activity normally results in a small proportion of active myonuclei replacement (1-2%) (117). We observed a proportion of 21.5% of cKO soleus myofibers displaying central nuclei (Illustration 9) while EDL muscle from the same animals showed only background levels (4.0%). Importantly, these animals were not subjected to conditions which would result in marked muscle damage such as inclined treadmill running. Genetic markers of muscle regeneration were found to be upregulated in the soleus muscles of 10 month old cKOs including *Myh3*, *Myl4*, and *Myf6* (Table 1). Embryonic myosin heavy chain isoforms such as *Myh3* and *Myl4* are expressed during

myofiber regeneration and fetal development, respectively (118, 119). *Myf6* encodes a myogenic regulatory transcription factor required for satellite cell activation, proliferation, and determination of myogenic fate (120). Thus cKO of *Mbtps1* in bone seems to be activating a slow-twitch muscle specific regeneration pathway.

Although mRNA profiling may explain the altered cKO soleus muscle phenotype, it is unknown how slow-twitch fibers are specifically targeted in this model. There is evidence that regulation of myogenesis occurs differently with respect to muscle fiber-type through the activation of discrete fast or slow twitch muscle –producing stem cell population (121). Additionally, primary satellite cells derived from soleus and EDL muscles behave differently within *in vitro* cell cultures with different proliferative and differentiation capabilities and responses to altered extracellular matrix compositions (122).

The reciprocal influences of bone-muscle endocrine/paracrine crosstalk may have significant impacts on bone and muscle health with respect to disease and aging processes. Indeed, muscle and bone quality are closely related. Sarcopenia and osteoporosis, the aging-related declines in muscle mass/function and bone density/strength, respectively, tend to occur concomitantly in the same individual (39). There is evidence that changes in pleiotropic genetics may play a role in musculoskeletal aging and disease which could affect normal secretory capacity and/or tissue responsiveness to secreted musculoskeletal factors (123, 124). Muscles and bone also influence each other in terms of tissue repair. Bone fracture healing is greatly improved with the application of vascularized muscle tissue flaps within the fracture area suggesting that local release of growth factors and/or stem cells from muscle may participate in normal healing and repair mechanisms (125-127).

Therefore, the development of efficacies which target musculoskeletal biochemical communication mechanisms may harbor great promise for treating a variety of musculoskeletal dysfunction in aging and disease.

In summary, with regards to muscle-to-bone or muscle-muscle crosstalk, we found that L-BAIBA is released from contracting skeletal muscles and that supplementation at 100mg/kg/day in mice during two weeks of hind limb unloading resulted in increased slow-twitch soleus muscle contractile force and rate of force development and reduced loss of trabecular bone content. These results highlight slow-twitch specific contractile effects of L-BAIBA and implicates L-BAIBA in muscle-to-bone endocrine crosstalk as an exercise metabolite that regulates bone structure. Next, with regards to bone-to-muscle crosstalk, we found that deletion of the protease, *Mbt�1*, in bone osteocytes resulted in a slow-twitch muscle phenotype characterized by actively regenerating type 1 myofibers and increased soleus muscle specific force and mass. Soleus muscle gene expression data correlated with observed structural and functional impacts. Bones were essentially normal in cKO mice indicating that musculoskeletal mechanical coupling is normal and that the effects in muscle are likely mediated by a novel *Mbt�1*-dependent bone-to-muscle endocrine crosstalk mechanism. Finally, these findings collectively underscore the humoral component and co-dependence of musculoskeletal health and physiology and its implications in aging and disease.

REFERENCES CITED

1. **Kuffler SW, Vaughan Williams EM.** 1953. Properties of the 'slow' skeletal muscles fibres of the frog. *J Physiol* **121**:318-340.
2. **Schiaffino S, Gorza L, Sartore S, Saggini L, Ausoni S, Vianello M, Gundersen K, Lomo T.** 1989. Three myosin heavy chain isoforms in type 2 skeletal muscle fibres. *J Muscle Res Cell Motil* **10**:197-205.
3. **Canepari M, Pellegrino MA, D'Antona G, Bottinelli R.** 2010. Skeletal muscle fibre diversity and the underlying mechanisms. *Acta Physiol (Oxf)* **199**:465-476.
4. **Bottinelli R, Schiaffino S, Reggiani C.** 1991. Force-velocity relations and myosin heavy chain isoform compositions of skinned fibres from rat skeletal muscle. *J Physiol* **437**:655-672.
5. **Weiss S, Rossi R, Pellegrino MA, Bottinelli R, Geeves MA.** 2001. Differing ADP release rates from myosin heavy chain isoforms define the shortening velocity of skeletal muscle fibers. *J Biol Chem* **276**:45902-45908.
6. **Stull JT, Kamm KE, Vandenberg R.** 2011. Myosin light chain kinase and the role of myosin light chain phosphorylation in skeletal muscle. *Arch Biochem Biophys* **510**:120-128.
7. **Schiaffino S, Reggiani C.** 1996. Molecular diversity of myofibrillar proteins: gene regulation and functional significance. *Physiol Rev* **76**:371-423.
8. **Zierath JR, Hawley JA.** 2004. Skeletal muscle fiber type: influence on contractile and metabolic properties. *PLoS Biol* **2**:e348.
9. **Wolff J.** 1892. Das Gesetz der Transformation der Knochen. Berlin, Germany: Verlag von August Hirschwald.
10. **Beno T, Yoon YJ, Cowin SC, Fritton SP.** 2006. Estimation of bone permeability using accurate microstructural measurements. *J Biomech* **39**:2378-2387.
11. **Tatsumi S, Ishii K, Amizuka N, Li M, Kobayashi T, Kohno K, Ito M, Takeshita S, Ikeda K.** 2007. Targeted ablation of osteocytes induces osteoporosis with defective mechanotransduction. *Cell Metab* **5**:464-475.
12. **Klein-Nulend J, van der Plas A, Semeins CM, Ajubi NE, Frangos JA, Nijweide PJ, Burger EH.** 1995. Sensitivity of osteocytes to biomechanical stress in vitro. *Faseb J* **9**:441-445.
13. **Ruggiu A, Cancedda R.** 2015. Bone mechanobiology, gravity and tissue engineering: effects and insights. *J Tissue Eng Regen Med* **9**:1339-1351.
14. **Globus RK, Morey-Holton E.** 1985. Hindlimb Unloading: Rodent Analog for Microgravity. *J Appl Physiol* **11**.
15. **Ohira T, Kawano F, Goto K, Ohira Y.** 2015. Responses of skeletal muscles to gravitational unloading and/or reloading. *J Physiol Sci* **65**:293-310.
16. **Thomason DB, Booth FW.** 1985. Atrophy of the soleus muscle by hindlimb unweighting. *J Appl Physiol* **68**:1-12.
17. **Baldwin KM, Haddad F.** 1985. Effects of different activity and inactivity paradigms on myosin heavy chain gene expression in striated muscle. *J Appl Physiol* **90**:345-357.
18. **Wagatsuma A, Kotake N, Kawachi T, Shiozuka M, Yamada S, Matsuda R.** 2011. Mitochondrial adaptations in skeletal muscle to hindlimb unloading. *Mol Cell Biochem* **350**:1-11.
19. **Feng HZ, Chen X, Malek MH, Jin JP.** 2016. Slow recovery of the impaired fatigue resistance in postunloading mouse soleus muscle corresponding to decreased mitochondrial function and a compensatory increase in type I slow fibers. *Am J Physiol Cell Physiol* **310**:7.

20. Riley DA, Slocum GR, Bain JL, Sedlak FR, Sowa TE, Mellender JW. 1985. Rat hindlimb unloading: soleus histochemistry, ultrastructure, and electromyography. *J Appl Physiol* **69**:58-66.
21. Mirzoev TM, Biriukov NS, Veselova OM, Larina IM, Shenkman BS, Ogneva IV. 2012. [Parameters of fibers cell respiration and desmin content in rat soleus muscle at early stages of gravitational unloading]. *Biofizika* **57**:509-514.
22. Yajid F, Mercier JG, Mercier BM, Dubouchaud H, Prefaut C. 1985. Effects of 4 wk of hindlimb suspension on skeletal muscle mitochondrial respiration in rats. *J Appl Physiol* **84**:479-485.
23. Lee IM, Shiroma EJ, Lobelo F, Puska P, Blair SN, Katzmarzyk PT. 2012. Effect of physical inactivity on major non-communicable diseases worldwide: an analysis of burden of disease and life expectancy. *Lancet* **380**:219-229.
24. Pedersen BK. 2009. The diseasome of physical inactivity--and the role of myokines in muscle--fat cross talk. *J Physiol* **587**:5559-5568.
25. Pedersen BK. 2011. Muscles and their myokines. *J Exp Biol* **214**:337-346.
26. Jeremic N, Chatuverdi P, Tyagi SC. 2016. Browning of White Fat: Novel Insight into Factors, Mechanisms and Therapeutics. *J Cell Physiol* doi:10.1002/jcp.25450.
27. Pedersen BK, Febbraio MA. 2008. Muscle as an endocrine organ: focus on muscle-derived interleukin-6. *Physiol Rev* **88**:1379-1406.
28. Bruunsgaard H, Galbo H, Halkjaer-Kristensen J, Johansen TL, MacLean DA, Pedersen BK. 1997. Exercise-induced increase in serum interleukin-6 in humans is related to muscle damage. *J Physiol* **499** (Pt 3):833-841.
29. Willoughby DS, McFarlin B, Bois C. 2003. Interleukin-6 expression after repeated bouts of eccentric exercise. *Int J Sports Med* **24**:15-21.
30. Carey AL, Steinberg GR, Macaulay SL, Thomas WG, Holmes AG, Ramm G, Prelovsek O, Hohnen-Behrens C, Watt MJ, James DE, Kemp BE, Pedersen BK, Febbraio MA. 2006. Interleukin-6 increases insulin-stimulated glucose disposal in humans and glucose uptake and fatty acid oxidation in vitro via AMP-activated protein kinase. *Diabetes* **55**:2688-2697.
31. Gleeson M. 2000. Interleukins and exercise. *J Physiol* **529 Pt 1**:1.
32. Ostrowski K, Rohde T, Asp S, Schjerling P, Pedersen BK. 1999. Pro- and anti-inflammatory cytokine balance in strenuous exercise in humans. *J Physiol* **515** (Pt 1):287-291.
33. Ostrowski K, Schjerling P, Pedersen BK. 2000. Physical activity and plasma interleukin-6 in humans--effect of intensity of exercise. *Eur J Appl Physiol* **83**:512-515.
34. Norrby K. 1996. Interleukin-8 and de novo mammalian angiogenesis. *Cell Prolif* **29**:315-323.
35. Nieman DC, Davis JM, Henson DA, Walberg-Rankin J, Shute M, Dumke CL, Utter AC, Vinci DM, Carson JA, Brown A, Lee WJ, McAnulty SR, McAnulty LS. 2003. Carbohydrate ingestion influences skeletal muscle cytokine mRNA and plasma cytokine levels after a 3-h run. *J Appl Physiol* (1985) **94**:1917-1925.
36. Haugen F, Norheim F, Lian H, Wensaas AJ, Dueland S, Berg O, Funderud A, Skalhegg BS, Raastad T, Drevon CA. 2010. IL-7 is expressed and secreted by human skeletal muscle cells. *Am J Physiol Cell Physiol* **298**:C807-816.
37. Quinn LS, Anderson BG, Drivdahl RH, Alvarez B, Argiles JM. 2002. Overexpression of interleukin-15 induces skeletal muscle hypertrophy in vitro: implications for treatment of muscle wasting disorders. *Exp Cell Res* **280**:55-63.
38. Quinn LS, Anderson BG, Strait-Bodey L, Stroud AM, Argiles JM. 2009. Oversecretion of interleukin-15 from skeletal muscle reduces adiposity. *Am J Physiol Endocrinol Metab* **296**:E191-202.

39. **Cianferotti L, Brandi ML.** 2014. Muscle-bone interactions: basic and clinical aspects. *Endocrine* **45**:165-177.
40. **Panati K, Suneetha Y, Narala VR.** 2016. Irisin/FNDC5 - An updated review. *Eur Rev Med Pharmacol Sci* **20**:689-697.
41. **Bostrom P, Wu J, Jedrychowski MP, Korde A, Ye L, Lo JC, Rasbach KA, Bostrom EA, Choi JH, Long JZ, Kajimura S, Zingaretti MC, Vind BF, Tu H, Cinti S, Hojlund K, Gygi SP, Spiegelman BM.** 2012. A PGC1-alpha-dependent myokine that drives brown-fat-like development of white fat and thermogenesis. *Nature* **481**:463-468.
42. **Colaianni G, Cuscito C, Mongelli T, Oranger A, Mori G, Brunetti G.** 2014. Irisin enhances osteoblast differentiation in vitro. *2014*:902186.
43. **Colaianni G, Cuscito C, Mongelli T, Pignataro P, Buccoliero C, Liu P, Lu P, Sartini L, Di Comite M, Mori G, Di Benedetto A, Brunetti G, Yuen T, Sun L, Reseland JE, Colucci S, New MI, Zaidi M, Cinti S, Grano M.** 2015. The myokine irisin increases cortical bone mass. *Proc Natl Acad Sci U S A* **112**:12157-12162.
44. **Maisonneuve C, Igoudjil A, Begriche K, Letteron P, Guimont MC, Bastin J, Laigneau JP, Pessayre D, Fromenty B.** 2004. Effects of zidovudine, stavudine and beta-aminoisobutyric acid on lipid homeostasis in mice: possible role in human fat wasting. *Antivir Ther* **9**:801-810.
45. **Begriche K, Massart J, Abbey-Toby A, Igoudjil A, Letteron P, Fromenty B.** 2008. Beta-aminoisobutyric acid prevents diet-induced obesity in mice with partial leptin deficiency. *Obesity (Silver Spring)* **16**:2053-2067.
46. **Roberts LD, Bostrom P, O'Sullivan JF, Schinzel RT, Lewis GD, Dejam A, Lee YK, Palma MJ, Calhoun S, Georgiadi A, Chen MH, Ramachandran VS, Larson MG, Bouchard C, Rankinen T, Souza AL, Clish CB, Wang TJ, Estall JL, Soukas AA, Cowan CA, Spiegelman BM, Gerszten RE.** 2014. beta-Aminoisobutyric acid induces browning of white fat and hepatic beta-oxidation and is inversely correlated with cardiometabolic risk factors. *Cell Metab* **19**:96-108.
47. **Shi CX, Zhao MX, Shu XD, Xiong XQ, Wang JJ, Gao XY, Chen Q, Li YH, Kang YM, Zhu GQ.** 2016. beta-aminoisobutyric acid attenuates hepatic endoplasmic reticulum stress and glucose/lipid metabolic disturbance in mice with type 2 diabetes. *Sci Rep* **6**:21924.
48. **Jung TW, Hwang HJ, Hong HC, Yoo HJ, Baik SH, Choi KM.** 2015. BAIBA attenuates insulin resistance and inflammation induced by palmitate or a high fat diet via an AMPK-PPARdelta-dependent pathway in mice. *Diabetologia* **58**:2096-2105.
49. **Dallas SL, Prideaux M, Bonewald LF.** 2013. The osteocyte: an endocrine cell ... and more. *Endocr Rev* **34**:658-690.
50. **Bonewald LF.** 2007. Osteocytes as dynamic multifunctional cells. *Ann N Y Acad Sci* **1116**:281-290.
51. **Vezeridis PS, Semeins CM, Chen Q, Klein-Nulend J.** 2006. Osteocytes subjected to pulsating fluid flow regulate osteoblast proliferation and differentiation. *Biochem Biophys Res Commun* **348**:1082-1088.
52. **Raisz LG, Fall PM, Gabbitas BY, McCarthy TL, Kream BE, Canalis E.** 1993. Effects of prostaglandin E2 on bone formation in cultured fetal rat calvariae: role of insulin-like growth factor-I. *Endocrinology* **133**:1504-1510.
53. **Jee WS, Ueno K, Deng YP, Woodbury DM.** 1985. The effects of prostaglandin E2 in growing rats: increased metaphyseal hard tissue and cortico-endosteal bone formation. *Calcif Tissue Int* **37**:148-157.
54. **Winkler DG, Sutherland MK, Geoghegan JC, Yu C, Hayes T, Skonier JE, Shpektor D, Jonas M, Kovacevich BR, Staehling-Hampton K, Appleby M, Brunkow ME, Latham JA.** 2003.

- Osteocyte control of bone formation via sclerostin, a novel BMP antagonist. *Embo J* **22**:6267-6276.
55. Li J, Sarosi I, Cattley RC, Pretorius J, Asuncion F, Grisanti M, Morony S, Adamu S, Geng Z, Qiu W, Kostenuik P, Lacey DL, Simonet WS, Bolon B, Qian X, Shalhoub V, Ominsky MS, Zhu Ke H, Li X, Richards WG. 2006. Dkk1-mediated inhibition of Wnt signaling in bone results in osteopenia. *Bone* **39**:754-766.
 56. Bodine PV, Zhao W, Kharode YP, Bex FJ, Lambert AJ, Goad MB, Gaur T, Stein GS, Lian JB, Komm BS. 2004. The Wnt antagonist secreted frizzled-related protein-1 is a negative regulator of trabecular bone formation in adult mice. *Mol Endocrinol* **18**:1222-1237.
 57. Zhao S, Zhang YK, Harris S, Ahuja SS, Bonewald LF. 2002. MLO-Y4 osteocyte-like cells support osteoclast formation and activation. *J Bone Miner Res* **17**:2068-2079.
 58. Shimada T, Kakitani M, Yamazaki Y, Hasegawa H, Takeuchi Y, Fujita T, Fukumoto S, Tomizuka K, Yamashita T. 2004. Targeted ablation of Fgf23 demonstrates an essential physiological role of FGF23 in phosphate and vitamin D metabolism. *J Clin Invest* **113**:561-568.
 59. Liu S, Tang W, Zhou J, Vierthalter L, Quarles LD. 2007. Distinct roles for intrinsic osteocyte abnormalities and systemic factors in regulation of FGF23 and bone mineralization in Hyp mice. *Am J Physiol Endocrinol Metab* **293**:E1636-1644.
 60. Schnedl C, Fahrleitner-Pammer A, Pietschmann P, Amrein K. 2015. FGF23 in Acute and Chronic Illness. *Dis Markers* **2015**:358086.
 61. Bonewald LF, Wacker MJ. 2013. FGF23 production by osteocytes. *Pediatr Nephrol* **28**:563-568.
 62. Touchberry CD, Green TM, Tchikrizov V, Mannix JE, Mao TF, Carney BW, Girgis M, Vincent RJ, Wetmore LA, Dawn B, Bonewald LF, Stubbs JR, Wacker MJ. 2013. FGF23 is a novel regulator of intracellular calcium and cardiac contractility in addition to cardiac hypertrophy. *Am J Physiol Endocrinol Metab* **304**:E863-873.
 63. Faul C, Amaral AP, Oskouei B, Hu MC, Sloan A, Isakova T, Gutierrez OM, Aguillon-Prada R, Lincoln J, Hare JM, Mundel P, Morales A, Scialla J, Fischer M, Soliman EZ, Chen J, Go AS, Rosas SE, Nessel L, Townsend RR, Feldman HI, St John Sutton M, Ojo A, Gadegbeku C, Di Marco GS, Reuter S, Kentrup D, Tiemann K, Brand M, Hill JA, Moe OW, Kuro OM, Kusek JW, Keane MG, Wolf M. 2011. FGF23 induces left ventricular hypertrophy. *J Clin Invest* **121**:4393-4408.
 64. Shen H, Grimston S, Civitelli R, Thomopoulos S. 2015. Deletion of connexin43 in osteoblasts/osteocytes leads to impaired muscle formation in mice. *J Bone Miner Res* **30**:596-605.
 65. Mo C, Romero-Suarez S, Bonewald L, Johnson M, Brotto M. 2012. Prostaglandin E2: from clinical applications to its potential role in bone- muscle crosstalk and myogenic differentiation. *Recent Pat Biotechnol* **6**:223-229.
 66. Seidah NG, Sadr MS, Chretien M, Mbikay M. 2013. The multifaceted proprotein convertases: their unique, redundant, complementary, and opposite functions. *J Biol Chem* **288**:21473-21481.
 67. Seidah NG, Prat A. 2012. The biology and therapeutic targeting of the proprotein convertases. *Nat Rev Drug Discov* **11**:367-383.
 68. Turpeinen H, Ortutay Z, Pesu M. 2013. Genetics of the first seven proprotein convertase enzymes in health and disease. *Curr Genomics* **14**:453-467.
 69. Seidah NG, Mowla SJ, Hamelin J, Mamarbachi AM, Benjannet S, Toure BB, Basak A, Munzer JS, Marcinkiewicz J, Zhong M, Barale JC, Lazure C, Murphy RA, Chretien M, Marcinkiewicz M. 1999. Mammalian subtilisin/kexin isozyme SKI-1: A widely expressed

- proprotein convertase with a unique cleavage specificity and cellular localization. *Proc Natl Acad Sci U S A* **96**:1321-1326.
70. **Sakai J, Rawson RB, Espenshade PJ, Cheng D, Seegmiller AC, Goldstein JL, Brown MS.** 1998. Molecular identification of the sterol-regulated luminal protease that cleaves SREBPs and controls lipid composition of animal cells. *Mol Cell* **2**:505-514.
 71. **Llarena M, Bailey D, Curtis H, O'Hare P.** 2010. Different mechanisms of recognition and ER retention by transmembrane transcription factors CREB-H and ATF6. *Traffic* **11**:48-69.
 72. **Patra D, Xing X, Davies S, Bryan J, Franz C, Hunziker EB, Sandell LJ.** 2007. Site-1 protease is essential for endochondral bone formation in mice. *J Cell Biol* **179**:687-700.
 73. **Achilleos A, Huffman NT, Marcinkiewicz E, Seidah NG, Chen Q, Dallas SL, Trainor PA, Gorski JP.** 2015. MBTPS1/SKI-1/S1P proprotein convertase is required for ECM signaling and axial elongation during somitogenesis and vertebral developmentdagger. *Hum Mol Genet* **24**:2884-2898.
 74. **Gorski JP, Huffman NT, Cui C, Henderson EP, Midura RJ, Seidah NG.** 2009. Potential role of proprotein convertase SKI-1 in the mineralization of primary bone. *Cells Tissues Organs* **189**:25-32.
 75. **Gorski JP, Huffman NT, Chittur S, Midura RJ, Black C, Oxford J, Seidah NG.** 2011. Inhibition of proprotein convertase SKI-1 blocks transcription of key extracellular matrix genes regulating osteoblastic mineralization. *J Biol Chem* **286**:1836-1849.
 76. **Gorski JP, Huffman NT, Vallejo J, Brotto L, Chittur SV, Breggia A, Stern A, Huang J, Mo C, Seidah NG, Bonewald L, Brotto M.** 2016. Deletion of Mbtps1 (Pcsk8, S1p, Ski-1) Gene in Osteocytes Stimulates Soleus Muscle Regeneration and Increased Size and Contractile Force with Age. *J Biol Chem* **291**:4308-4322.
 77. **Jahn K, Lara-Castillo N, Brotto L, Mo CL, Johnson ML, Brotto M, Bonewald LF.** 2012. Skeletal muscle secreted factors prevent glucocorticoid-induced osteocyte apoptosis through activation of beta-catenin. *Eur Cell Mater* **24**:197-209; discussion 209-110.
 78. **Park KH, Brotto L, Lehoang O, Brotto M, Ma J, Zhao X.** 2012. Ex vivo assessment of contractility, fatigability and alternans in isolated skeletal muscles. *J Vis Exp* doi:10.3791/4198:e4198.
 79. **Putty S, Vemula H, Bobba S, Gutheil WG.** 2013. A liquid chromatography-tandem mass spectrometry assay for d-Ala-d-Lac: a key intermediate for vancomycin resistance in vancomycin-resistant enterococci. *Anal Biochem* **442**:166-171.
 80. **Jamindar D, Gutheil WG.** 2010. A liquid chromatography-tandem mass spectrometry assay for Marfey's derivatives of L-Ala, D-Ala, and D-Ala-D-Ala: application to the in vivo confirmation of alanine racemase as the target of cycloserine in Escherichia coli. *Anal Biochem* **396**:1-7.
 81. **Brotto MA, Nosek TM, Kolbeck RC.** 2002. Influence of ageing on the fatigability of isolated mouse skeletal muscles from mature and aged mice. *Exp Physiol* **87**:77-82.
 82. **Yang J, Goldstein JL, Hammer RE, Moon YA, Brown MS, Horton JD.** 2001. Decreased lipid synthesis in livers of mice with disrupted Site-1 protease gene. *Proc Natl Acad Sci U S A* **98**:13607-13612.
 83. **Lu Y, Xie Y, Zhang S, Dusevich V, Bonewald LF, Feng JQ.** 2007. DMP1-targeted Cre expression in odontoblasts and osteocytes. *J Dent Res* **86**:320-325.
 84. **Phillips CL, Yamakawa K, Adelstein RS.** 1995. Cloning of the cDNA encoding human nonmuscle myosin heavy chain-B and analysis of human tissues with isoform-specific antibodies. *J Muscle Res Cell Motil* **16**:379-389.

85. **Judex S, Zhang W, Donahue LR, Ozcivici E.** 2013. Genetic loci that control the loss and regain of trabecular bone during unloading and reambulation. *J Bone Miner Res* **28**:1537-1549.
86. **Sartore S, Gorza L, Schiaffino S.** 1982. Fetal myosin heavy chains in regenerating muscle. *Nature* **298**:294-296.
87. **Burguiere AC, Nord H, von Hofsten J.** 2011. Alkali-like myosin light chain-1 (myl1) is an early marker for differentiating fast muscle cells in zebrafish. *Dev Dyn* **240**:1856-1863.
88. **DeChiara TM, Bowen DC, Valenzuela DM, Simmons MV, Poueymirou WT, Thomas S, Kinetz E, Compton DL, Rojas E, Park JS, Smith C, DiStefano PS, Glass DJ, Burden SJ, Yancopoulos GD.** 1996. The receptor tyrosine kinase MuSK is required for neuromuscular junction formation in vivo. *Cell* **85**:501-512.
89. **Uno M, Nishimura S, Fukuchi K, Kaneta Y, Oda Y, Komori H, Takeda S, Haga T, Agatsuma T, Nara F.** 2012. Identification of physiologically active substances as novel ligands for MRGPRD. *J Biomed Biotechnol* **2012**:816159.
90. **Etelvino GM, Peluso AA, Santos RA.** 2014. New components of the renin-angiotensin system: alamandine and the MAS-related G protein-coupled receptor D. *Curr Hypertens Rep* **16**:433.
91. **Shinohara T, Harada M, Ogi K, Maruyama M, Fujii R, Tanaka H, Fukusumi S, Komatsu H, Hosoya M, Noguchi Y, Watanabe T, Moriya T, Itoh Y, Hinuma S.** 2004. Identification of a G protein-coupled receptor specifically responsive to beta-alanine. *J Biol Chem* **279**:23559-23564.
92. **Edwards RH, Hill DK, Jones DA, Merton PA.** 1977. Fatigue of long duration in human skeletal muscle after exercise. *J Physiol* **272**:769-778.
93. **Stephenson DG, Williams DA.** 1981. Calcium-activated force responses in fast- and slow-twitch skinned muscle fibres of the rat at different temperatures. *J Physiol* **317**:281-302.
94. **Kang H, Viollet B, Wu D.** 2013. Genetic deletion of catalytic subunits of AMP-activated protein kinase increases osteoclasts and reduces bone mass in young adult mice. *J Biol Chem* **288**:12187-12196.
95. **Shah M, Kola B, Bataveljic A, Arnett TR, Viollet B, Saxon L, Korbonits M, Chenu C.** 2010. AMP-activated protein kinase (AMPK) activation regulates in vitro bone formation and bone mass. *Bone* **47**:309-319.
96. **Ichinoseki-Sekine N, Yoshihara T, Kakigi R, Ogura Y, Sugiura T, Naito H.** 2012. Fiber-type specific expression of alpha-actinin isoforms in rat skeletal muscle. *Biochem Biophys Res Commun* **419**:401-404.
97. **Ogura Y, Naito H, Kakigi R, Akema T, Sugiura T, Katamoto S, Aoki J.** 2009. Different adaptations of alpha-actinin isoforms to exercise training in rat skeletal muscles. *Acta Physiol (Oxf)* **196**:341-349.
98. **Ogura Y, Naito H, Kakigi R, Ichinoseki-Sekine N, Kurosaka M, Yoshihara T, Akema T.** 2011. Effects of ageing and endurance exercise training on alpha-actinin isoforms in rat plantaris muscle. *Acta Physiol (Oxf)* **202**:683-690.
99. **Paulin D, Li Z.** 2004. Desmin: a major intermediate filament protein essential for the structural integrity and function of muscle. *Exp Cell Res* **301**:1-7.
100. **Agbulut O, Li Z, Perie S, Ludosky MA, Paulin D, Cartaud J, Butler-Browne G.** 2001. Lack of desmin results in abortive muscle regeneration and modifications in synaptic structure. *Cell Motil Cytoskeleton* **49**:51-66.
101. **Wieneke S, Stehle R, Li Z, Jockusch H.** 2000. Generation of tension by skinned fibers and intact skeletal muscles from desmin-deficient mice. *Biochem Biophys Res Commun* **278**:419-425.

102. **Anderson J, Li Z, Goubel F.** 2002. Models of skeletal muscle to explain the increase in passive stiffness in desmin knockout muscle. *J Biomech* **35**:1315-1324.
103. **Balogh J, Li Z, Paulin D, Arner A.** 2003. Lower active force generation and improved fatigue resistance in skeletal muscle from desmin deficient mice. *J Muscle Res Cell Motil* **24**:453-459.
104. **Valenzuela DM, Stitt TN, DiStefano PS, Rojas E, Mattsson K, Compton DL, Nunez L, Park JS, Stark JL, Gies DR, et al.** 1995. Receptor tyrosine kinase specific for the skeletal muscle lineage: expression in embryonic muscle, at the neuromuscular junction, and after injury. *Neuron* **15**:573-584.
105. **Chevessier F, Girard E, Molgo J, Bartling S, Koenig J, Hantai D, Witzemann V.** 2008. A mouse model for congenital myasthenic syndrome due to MuSK mutations reveals defects in structure and function of neuromuscular junctions. *Hum Mol Genet* **17**:3577-3595.
106. **Close R.** 1964. DYNAMIC PROPERTIES OF FAST AND SLOW SKELETAL MUSCLES OF THE RAT DURING DEVELOPMENT. *J Physiol* **173**:74-95.
107. **Zhao X, Weisleder N, Thornton A, Oppong Y, Campbell R, Ma J, Brotto M.** 2008. Compromised store-operated Ca²⁺ entry in aged skeletal muscle. *Aging Cell* **7**:561-568.
108. **Brotto MA, Nagaraj RY, Brotto LS, Takeshima H, Ma JJ, Nosek TM.** 2004. Defective maintenance of intracellular Ca²⁺ homeostasis is linked to increased muscle fatigability in the MG29 null mice. *Cell Res* **14**:373-378.
109. **Nishi M, Komazaki S, Kurebayashi N, Ogawa Y, Noda T, Iino M, Takeshima H.** 1999. Abnormal features in skeletal muscle from mice lacking mitsugumin29. *J Cell Biol* **147**:1473-1480.
110. **Zhao X, Yoshida M, Brotto L, Takeshima H, Weisleder N, Hirata Y, Nosek TM, Ma J, Brotto M.** 2005. Enhanced resistance to fatigue and altered calcium handling properties of sarcalumenin knockout mice. *Physiol Genomics* **23**:72-78.
111. **Matzuk MM, Lu N, Vogel H, Sellheyer K, Roop DR, Bradley A.** 1995. Multiple defects and perinatal death in mice deficient in follistatin. *Nature* **374**:360-363.
112. **Amthor H, Nicholas G, McKinnell I, Kemp CF, Sharma M, Kambadur R, Patel K.** 2004. Follistatin complexes Myostatin and antagonises Myostatin-mediated inhibition of myogenesis. *Dev Biol* **270**:19-30.
113. **Winbanks CE, Weeks KL, Thomson RE, Sepulveda PV, Beyer C, Qian H, Chen JL, Allen JM, Lancaster GI, Febbraio MA, Harrison CA, McMullen JR, Chamberlain JS, Gregorevic P.** 2012. Follistatin-mediated skeletal muscle hypertrophy is regulated by Smad3 and mTOR independently of myostatin. *J Cell Biol* **197**:997-1008.
114. **Lee SJ, Lee YS, Zimmers TA, Soleimani A, Matzuk MM, Tsuchida K, Cohn RD, Barton ER.** 2010. Regulation of muscle mass by follistatin and activins. *Mol Endocrinol* **24**:1998-2008.
115. **Haidet AM, Rizo L, Handy C, Umapathi P, Eagle A, Shilling C, Boue D, Martin PT, Sahenk Z, Mendell JR, Kaspar BK.** 2008. Long-term enhancement of skeletal muscle mass and strength by single gene administration of myostatin inhibitors. *Proc Natl Acad Sci U S A* **105**:4318-4322.
116. **Charge SB, Rudnicki MA.** 2004. Cellular and molecular regulation of muscle regeneration. *Physiol Rev* **84**:209-238.
117. **Schmalbruch H, Lewis DM.** 2000. Dynamics of nuclei of muscle fibers and connective tissue cells in normal and denervated rat muscles. *Muscle Nerve* **23**:617-626.
118. **Mathes AL, Lafyatis R.** 2011. Role for Toll-like receptor 3 in muscle regeneration after cardiotoxin injury. *Muscle Nerve* **43**:733-740.
119. **Hernandez OM, Jones M, Guzman G, Szczesna-Cordary D.** 2007. Myosin essential light chain in health and disease. *Am J Physiol Heart Circ Physiol* **292**:H1643-1654.

120. **Rudnicki MA, Le Grand F, McKinnell I, Kuang S.** 2008. The molecular regulation of muscle stem cell function. *Cold Spring Harb Symp Quant Biol* **73**:323-331.
121. **Kalhovde JM, Jerkovic R, Sefländ I, Cordonnier C, Calabria E, Schiaffino S, Lomo T.** 2005. "Fast" and "slow" muscle fibres in hindlimb muscles of adult rats regenerate from intrinsically different satellite cells. *J Physiol* **562**:847-857.
122. **Lagord C, Soulet L, Bonavaud S, Bassaglia Y, Rey C, Barlovatz-Meimon G, Gautron J, Martelly I.** 1998. Differential myogenicity of satellite cells isolated from extensor digitorum longus (EDL) and soleus rat muscles revealed in vitro. *Cell Tissue Res* **291**:455-468.
123. **Karasik D, Kiel DP.** 2010. Evidence for pleiotropic factors in genetics of the musculoskeletal system. *Bone* **46**:1226-1237.
124. **Karasik D, Cohen-Zinder M.** 2012. The genetic pleiotropy of musculoskeletal aging. *Front Physiol* **3**:303.
125. **Gopal S, Majumder S, Batchelor AG, Knight SL, De Boer P, Smith RM.** 2000. Fix and flap: the radical orthopaedic and plastic treatment of severe open fractures of the tibia. *J Bone Joint Surg Br* **82**:959-966.
126. **Schindeler A, Liu R, Little DG.** 2009. The contribution of different cell lineages to bone repair: exploring a role for muscle stem cells. *Differentiation* **77**:12-18.
127. **Liu R, Schindeler A, Little DG.** 2010. The potential role of muscle in bone repair. *J Musculoskelet Neuronal Interact* **10**:71-76.

VITA

Julian Alfredo Vallejo was born in Austin, Texas on the 20th of July, 1987. He attended Liberty High School in Liberty, Missouri and graduated in 2006. During high school, Mr. Vallejo completed the A+ Scholarship Program and received a scholarship to the Metropolitan Community College system where he completed of two years of study in Biology. He then transferred to the University of Missouri-Kansas City where he completed additional coursework in Biological Sciences and was awarded the Bachelor of Science in Biology Degree in 2011.

After graduation, Mr. Vallejo volunteered in the skeletal muscle research laboratory of Dr. Marco Brotto and assumed a position as Research Assistant in 2012. As a Research Assistant, Mr. Vallejo learned molecular, cellular and animal dissection techniques, and provided contributions to various research projects. Through his work Mr. Vallejo attained co-authorship on several research publications including: **Garimella R. *Trans Oncol.* 2014, Mo C. *Cell Cycle.* 2015** and **Gorski JP. *J Biol Chem.* 2016.** In 2013 Mr. Vallejo was awarded an NIH Diversity Supplement Grant to pursue a Master of Science in Cellular and Molecular Biology Degree from UMKC while continuing to perform laboratory research.

In 2016, Mr. Vallejo published a first author manuscript entitled, “Cellular and Physiological Effects of Dietary Supplementation with β -hydroxy- β -methylbutyrate (HMB) and β -alanine in Late Middle-Aged Mice” in the journal PlosOne. Upon completion of his research in the laboratory of Dr. Marco Brotto, Mr. Vallejo next assumed a Research Assistant position in the bone research laboratory of Dr. Lynda Bonewald to continue studying skeletal muscle and its involvement in bone-muscle endocrine crosstalk. After completion of his degree requirements, Mr. Vallejo plans to continue his career in basic laboratory research.